Critical habitats of Arctic grayling in Parsnip tributaries

Fish and Wildlife Compensation Program
Peace Project No. PEA-F23-F-3652

Prepared for:
Fish and Wildlife Compensation Program – Peace
3333 22nd Ave
Prince George, BC
V2N 1B4

Prepared by:
Joseph R. Bottoms, Eduardo G. Martins, Avery Dextrase, Marie Auger-Methé, and Christopher More O'Ferrall

University of Northern British Columbia
3333 University Way
Prince George, BC
V2N 4Z9

Prepared with financial support of the Fish and Wildlife Compensation Program on behalf of its program partners BC Hydro, the Province of BC, Fisheries and Oceans Canada, First Nations and Public Stakeholders.

29-September-2023

Table of Contents

List of Figures

List of Tables

Executive Summary

The research carried out in this report sought to answer questions about the critical habitat use of Arctic grayling during their summer rearing periods in the Anzac River. We examined the questions of which physical and thermal habitat types Arctic grayling selected for during their critical summer rearing period and investigated how these habitats were distributed at the riverscape scale. We also examined the questions of how effectively Arctic grayling regulate their body temperatures in thermally patchy riverine habitats, and whether these behaviors were energetically costly to maintain. We approached these questions with integrated modeling approaches using multiscale data collected with drones, snorkel surveys, temperature logger arrays, biologging with radio telemetry, and shuttlebox experiments. The methods applied in this work address overarching objectives related to Action #9 in the Rivers, Lakes, and Reservoirs Action Plan (PEA.RLR.S03.RI.09; Conduct research and monitoring of Arctic grayling) and subobjectives described both therein and within this report.

This work produced a suite of ecological data examining the Anzac River Arctic grayling during their summer rearing period from July-September 2022. Two study reaches of approximately 2 km in length were mapped temporally over four dates producing eight sets of grouped GIS layers delineating physical habitats and the spatial distribution of surface heat signatures. A riverscape-scale survey was also conducted, producing a continuous physical and thermal map of the first 52 kilometers of the Anzac River that can be used by resource managers for fine-scale conservation planning. At both the reach-scale and the riverscape-scales, snorkel surveys showed associations between Arctic grayling occurrence and cool pool habitats. Animations of hourly temperatures within the two study reaches were compiled, highlighting the spatial importance of pools as thermal refugia during temperature extreme events. An index of pool habitats was created at the riverscape scale to produce general maps of critical rearing habitat distributions within the Anzac River. River reaches between river kilometers 7-8, 11-15, 17-18, 22-28, 32-34, 37-39, and 44-48 were all identified as areas of high conservation potential within the riverscape as they contained high quality Arctic grayling physical and thermal habitats relative to the reaches around them.

To estimate metrics related to *in-situ* thermal habitat use and behavioral thermoregulation in Arctic grayling, two sets of controlled shuttlebox experiments were conducted. These experiments produced metrics of Arctic grayling thermal preference (T_{PREF} = 11.6 °C), preferred thermal range (T_{SET} = 10.1 - 13.0 °C), and a metric of the rate of heat transfer between external temperatures and internal body temperatures (k = 0.0013). These metrics were used to analyze both thermal habitat use and energy expenditure data collected from 50 free-ranging Arctic grayling tagged with radio transmitters. Analyses revealed that Arctic grayling most carefully behaviorally thermoregulate when ambient water temperatures exceed their T_{SET} range at the hottest parts of the day, and that this behavioral strategy was energetically costly to maintain (as revealed by activity data). A behavioral

change was observed after September 4, when ambient temperatures dropped below the T_{SET} range and Arctic grayling switched from active behavioral thermoregulation during the day to thermoregulating at night.

We used resource selection probability functions to reveal strong associations between Arctic grayling and pool habitats in our drone and snorkel surveys. Through our radio tagging work, we found that Arctic grayling are efficient behavioral thermoregulators when ambient temperatures are just beyond their preferred temperature range, but this behavior is costly to maintain and is a function of additive effects of temperature, hour of the day, energy expenditure, patchiness of the thermal habitat, and fish body condition. We also predicted that the extents of these preferable Anzac River thermal habitats will decrease with climate warming. We base our recommendations on the risks that Arctic grayling are likely to face in the coming years: (1) Where possible, explore management strategies to reduce angling pressures on Arctic grayling during thermal extremes, (2) implement educational signage in the Anzac River informing anglers about the potential detrimental effects of exercising fish with the capture process during thermal extremes, (3) develop a long-term index of thermal habitat quality in the Anzac that can be efficiently and repeatedly conducted in this system over five to ten-year intervals, and (4) extend the methods used in this study to examine the Table River to create a more complete picture of Arctic grayling habitat use and availability in the Parsnip River watershed. We also broadly recommend that these data support future conservation actions in the watershed.

1. Introduction

The 1967 completion of the WAC Bennett Dam and impoundment of the Williston Reservoir led to significant habitat loss for the region's fluvial Arctic grayling (*Thymallus arcticus*) population by converting extensive areas of riverine habitats into deeper, slower, more lake-like habitats unsuited to this stream-adapted population (Stamford et al. 2017, Lashmar and Ptolemy 2002, Stamford 2002). The effects of habitat loss were compounded by overfishing as anglers exploring the ever-expanding network of resource roads gained access to new Arctic grayling habitats which were previously remote (Lashmar and Ptolemy 2002). By 1995, a harvest moratorium was imposed on the Williston watershed Arctic grayling following their designation as a red-listed population. The use of Conservation Units in British Columbia was in its infancy in 1995, and as the program matured and genetic designation criteria became established, the Williston Arctic grayling were reclassified as part of the greater Southern Beringean genetic lineage and were moved to the yellow-list ca. 2002 (M. Stamford, Stamford Environmental; S. Pollard, Freshwater Fisheries Society of B.C. *Personal Communications*). Though the harvest moratorium remains today, special considerations must be taken to develop a conservation plan for the Williston fluvial Arctic grayling, which are now separated from the rest of the Southern Beringean lineage by the Williston Reservoir.

The habitat areas necessary for the conservation of a species – a species' *critical habitat* – are geographically diffuse across the landscape. This is particularly true of migratory species, whose habitat requirements can vary significantly both seasonally and within the lifespan of an individual (Chapman et al. 2012; Elsner & Shrimpton 2019). Identifying critical habitats and when/how individuals in a population access and use them are key considerations for conservation practitioners seeking to create an action plan for the management and recovery of a species (Cooke et al. 2016). Indeed, a recent review and monitoring framework by Hagen and Stamford (2017) highlighted a number of critical information gaps related to the critical habitats of migratory Arctic grayling (*Thymallus arcticus)* in the Williston Reservoir Watershed that must be addressed before on-the-ground enhancement and conservation actions can be initiated with support from the Fish and Wildlife Compensation Program. For example, within the high-priority data gaps regarding the unknown distribution of Arctic grayling within core areas, the authors list the delineation of critical habitats as 'essential' for identifying (1) potential threats to Arctic grayling populations, (2) potential limiting factors for each life stage, (3) appropriate locations for conservation or enhancement activity, and (4) life histories within a core area (Stamford et al. 2017).

Determining the appropriate scale to conduct effective studies linking fish ecology in rivers to conservation has been one of the main topics in a body of literature known as riverscape ecology. Riverscapes are relatively narrow corridors of habitat that cut, meander, or braid across the larger landscape (Torgersen et al. 2021; Fausch et al. 2002). The processes that drive the abundance and distribution of organisms within riverscapes are often multiscale – that is, they are dependent on both the reach-scale heterogeneity of the rivers themselves (Hughes 1998; Sears et al. 2019) and the context of the large-scale landscape through which

they flow (Morash et al. 2020). Studies at the reach-scale (10s – 1000s m) may be useful for examining fish behaviour or physiology, but they often lack the context of (and thus applicability to) the greater riverscape. Studies at the riverscape-scale (10s – 100s of km) may be useful for watershed management purposes, but discrete habitat features (e.g. thermal refugia associated with groundwater upwelling zones) may be lost to the coarse resolution (Dzara et al. 2019). Indeed, the identification of Arctic grayling critical habitats within the Williston watershed must be conducted at a scale useful to conservation practitioners (< 1-10 km; Hagen and Stamford 2017, Stamford et al. 2017), while the connectivity of these critical habitats across the riverscape must be examined at a scale sufficient to identify limiting factors that Arctic grayling may encounter along their annual migration routes and feeding, spawning, and overwintering seasonal habitats (10s – 100s of km; Dzara et al. 2019; Blackman 2002).

Riverscapes also demonstrate multiscale processes with respect to time, exhibiting variability in the short-term (e.g daily thermal cycles), intermediate-term (e.g. seasonal hydrological and thermal cycles), and in some cases in the long-term (e.g. annual and interannual shifts in the course of the riverscape itself) (Stanford et al. 2005). Responses of freshwater fishes to changes in the riverscape, particularly those with long temporal scales (e.g. climate change), or those related to discrete events (land use changes) or persistent events (interruption to connectivity), may be best understood within the context of their responses across fine temporal scales (Wolkovich et al. 2014). For example, historic (long-term) river temperatures are connected to modern thermal optimums in populations of salmonids, and their responses to temperature extremes in excess of these optimums is both cumulative (on a daily scale) and proportionate to the magnitude and duration (a relatively fine-scale) of the thermal stress (Farrell et al. 2008; Rezende et al. 2014). As climate change forces more frequent and more severe extreme temperature events (like the heat dome in June of 2021), the behavioural and physiological responses of Arctic grayling will be related to the availability of thermally heterogeneous habitats in which individuals can effectively thermoregulate and recover across fine temporal scales (Wolkovich et al. 2014; Farrell et al. 2008).

Temperature has the strong potential to limit Arctic grayling populations in the Williston Reservoir watershed (Stamford et al. 2017). As the reservoir watershed is located at the southern periphery of the species' distribution at the Arctic Divide in north-central British Columbia, this population may be particularly susceptible to the impacts of climate change (Vatland et al. 2015; Troia et al. 2019). The impacts of temperature on the ecophysiology of freshwater fishes are well documented; it can act as a cue for migration (Elsner & Shrimpton 2019), dictate the times conducive to (and intensity of) activity (Abram et al. 2017), and extreme temperatures can trigger mass mortality events in cold-water salmonids (Martins et al. 2011). Populations adapt to changes in the thermal environment over years to decades through selective pressures on their underlying genetics. In contrast, individuals adapt to their thermal environment in the mid-term (days to months) through physiological acclimation (Sears et al. 2019), but over the short-term (seconds to minutes) must rely on behavioral thermoregulation (i.e. seeking out cooler or warmer habitat) to

regulate their body temperatures around a thermal optimum and avoid critical temperature extremes (Farrell et al. 2008).

Although temperature is largely considered to be the most important variable determining habitat use and the distribution of fish across the riverscape, temperature alone is not enough to accurately predict Arctic grayling habitat use and distribution in rivers. The energetic costs associated with behavioral thermoregulation – the currency with which Arctic grayling navigate the tradeoffs presented by their environments – are dependent on the availability of critical feeding habitats across the riverscape (Hughes 1998). Feeding hierarchies in which adult and subadult Arctic grayling position themselves to maximize their energy income (Hughes 1999) are centered around pool habitats (McPhail 2007), which are heterogeneous in space (and on a longer-scale, in time) in the Anzac and Table rivers. Riverscape-scale distributions are connected to age and size-dependent movement (Hughes 1999), which are related to flow and availability of flow refugia across the riverscape. Mechanisms related to habitat degradation, particularly levels of sediment transport, are considered important limiting factors to Arctic grayling during their summer migrations Rearing adults are highly reliant on sight for feeding and will migrate away from areas of high turbidity to find different feeding habitats (Stamford et al. 2017). At all habitats and life history stages, the presence of antagonistic species such as potential predators (e.g. bull trout *Salvelinus confluentus*) or competitors (e.g. mountain whitefish *Prosopium williamsoni*) may also influence how effectively Arctic grayling are able to locate and use their critical thermal and physical habitats.

2. Objectives and Linkages to FWCP Action Plans and Priority Areas

This project had four primary objectives: to (1) conduct a continuous riverscape survey using a multiscale, nested design (*sensu* Fausch 2002) to identify critical thermal and physical habitats in the Anzac riverscape (to the extent where Arctic grayling occurrence is not limited by barriers); (2) identify factors that may impact Arctic grayling access to, or use of, critical thermal or physical habitats in the Anzac River; (3) quantify the costs of behavioural thermoregulation in free-ranging Arctic grayling moving within and among critical habitats in the presence and absence of potential predators (bull trout) and/or competitors (mountain whitefish); and (4) forecast how further cumulative changes to the riverscapes through mechanisms related to climate change and land use change may alter the extents of Arctic grayling critical habitats.

These objectives were explored using a combination of field- and laboratory-based methods and results were compiled into a visualization format useful to fishery managers and conservation practitioners using Geographic Information Systems (GIS) software. This research addressed Action #9 in the Rivers, Lakes, and Reservoirs Action Plan (PEA.RLR.S03.RI.09 *Conduct research and monitoring of Arctic grayling*). Specifically, this study addressed the monitoring needs associated with priority information Gap 3 in Table 1 of Hagen & Stamford (2017; *Lack of assessment of aquatic ecosystem health - habitat*

threats; Monitoring need: GIS indicator-based assessment of aquatic ecosystem health; Fish Habitat Assessment Procedures), as well as integrated aspects of Steps 1 - 3 of the associated monitoring sequence outlined in section 2.2 of their report (***Step 1****: Acquire population data (abundance, trend, distribution) and indicators of aquatic ecosystem health (threats) for the purposes of: 1) delineating critical habitats 2) assessing conservation status (and the need for conservation and enhancement actions), 3) prioritizing among candidate locations for conservation and enhancement actions, and 4) establishing a quantitative baseline for effectiveness monitoring*; ***Step 2:*** *Identify critical habitats utilized by key Arctic Grayling life stages, at the level of geographic accuracy suitable for delineating conservation and enhancement actions (e.g. ± 1 km)*; and ***Step 3:*** *Assess potential limiting factors (see preceding section) operating within critical habitats, in order to design and initiate conservation and enhancement actions*).

3. Study Area

The Anzac River is a major tributary of the Parsnip River and has a course of 78 km from headwaters at 2,495 m to its confluence with the Parsnip at 730 m. Together with the Table River, it serves as an important hub for Arctic grayling populations in the region (Stamford et al. 2017). The river drains a mountainous region of the Hart Ranges in the Rocky Mountains and has a catchment area of 939 km^2. The upper river is characterized by bedrock canyons with a moderate gradient (1 - 2%) which reduces to low-gradient meanders across the wide lower river valley as it nears the Parsnip River confluence. Spring freshet in this system is dramatic; snowmelt causes high flows and turbidity which peak soon after ice out and then by late summer gradually reduce to low and clear conditions that persist into the fall.

This study occurred across two spatial scales. The Anzac riverscape survey (mapping of thermal and physical habitats as well as snorkel surveys for population abundance) happened over three days in August and simultaneously represents the largest spatial scale and the smallest temporal scale of the study. Biweekly surveys for both the drone mapping and snorkel surveys as well as a biologging radio telemetry study were conducted at the reach scale on two selected study reaches of 1.2 and 2 km. The two reaches were selected based on a combination of site accessibility for regular tagging and snorkeling access, heterogeneity of available thermal habitats within the reach (i.e., tributary inputs and habitats of varying depths and feature classes), and topology amenable to radio receiver line-of-sight.

Reach A, the lower of the two reaches, was a 2 km reach defined from river kilometers (Rkm) 35 - 37 (Figure 1). It features two small tributary inputs, the lower of which enters the Anzac at temperatures warmer than mainstem temperatures after flowing through areas of clearcut land use. The elevation at the center of the reach is 797 m. Habitats in reach A were varied, including cobble-boulder pools along a bedrock shelf, a long shallow run over bedrock substrates, a prominent deep corner pool, river braids around instream islands, and multiple series of riffle-pool interfaces. A long section of shallow riffles and micro-pools spans through the lower parts of the reach before opening to small shallow

pools and tailing out of the study area. Reach B, the upper of the two reaches, was a 1.1 km reach defined from Rkm 46.5 - 47.6 (Figure 2). It featured a major tributary input which supported Arctic grayling use in the lower 100 m, a major bedrock chute and series of rapids, series of cobble riffles and pools, a prominent plunge pool below the chute, and a prominent feeding pool below the tributary confluence. The elevation at the center of reach B is 856 m. Both reaches included a bridge across the mainstem Anzac River.

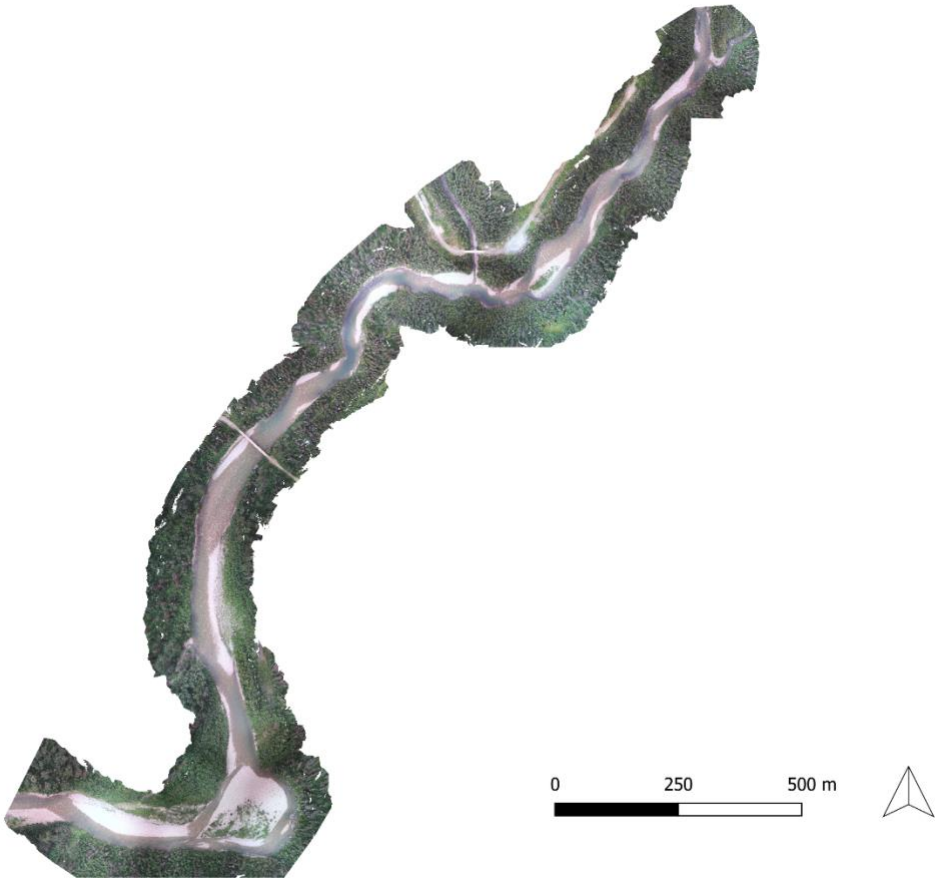

Figure 1. Study reach "A" from Rkm 35 - 37. A 1.7 km centrally located subsection was used in snorkel surveys (visible in figure 18).

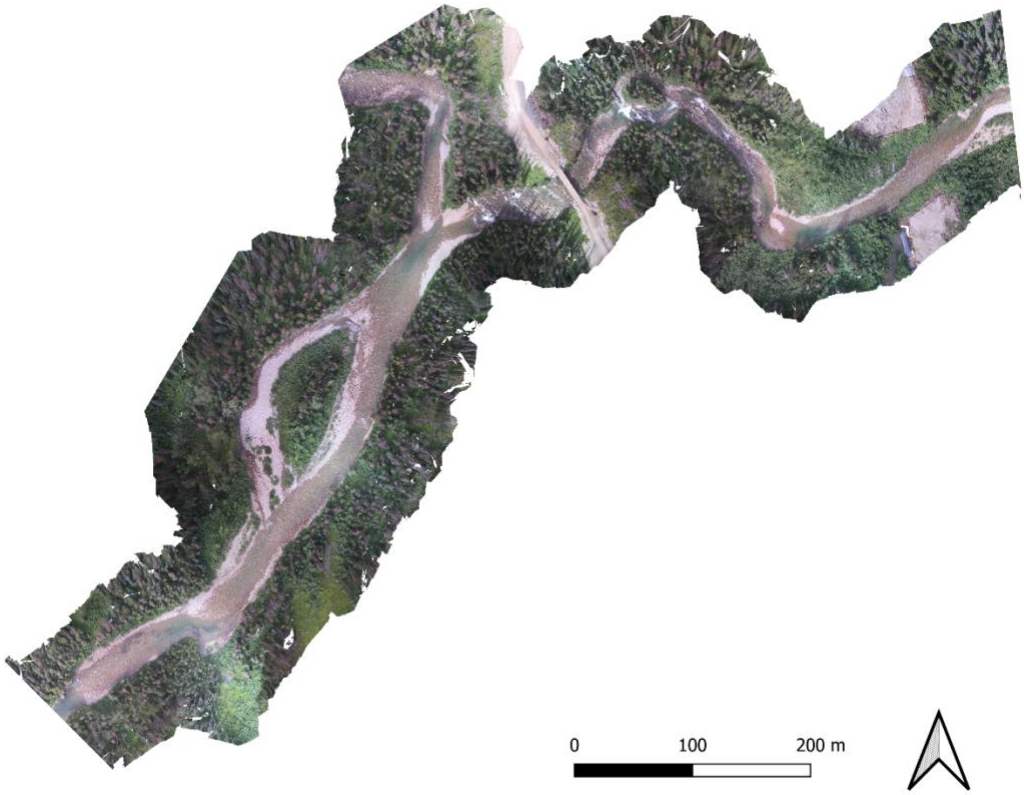

Figure 2. Study reach "B" from Rkm 46.5 - 47.6. A 1.1 km subsection was used in the snorkel surveys (visible in Figure 19). The CGL pipeline right-of-way crosses underneath the Eastern periphery of the reach.

4. Methods

Methods used in this report are classified following a general organizational structure around habitat use, habitat availability, and habitat preferences. The methods were applied to describe a complex ecological relationship and metrics and data derived from each objective were used in the analyses for other objectives. A general description of the interface between the three organizational structures of data collection is given in Figure 3.

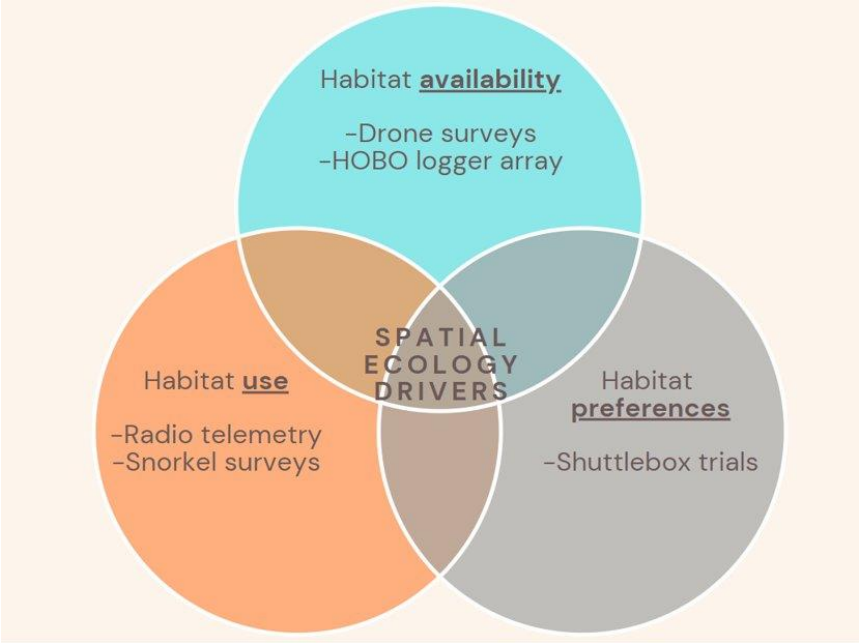

Figure 3. Methodological organization of this study.

While the methodology fell into discrete categories relevant to behavioral studies, the workflow for the analyses is best presented by methodological categories organized by data structures which grouped well together. Analyses were broken into three components: 1) biweekly drone and snorkel surveys (which occurred on the same dates) to assess the spatiotemporal distribution of Arctic grayling with their physical and thermal habitats; 2) shuttlebox experiments (which were all done in a laboratory setting) to determine the thermal preference range and rate of heat transfer in Arctic grayling; and 3) biologging with radio telemetry (which was done continuously between July 31 and September 15) to determine the effectiveness of behavioural regulation. The Methods, Results and Outcomes, and Discussion sections all follow this organizational structure.

Drone and snorkel surveys

To assess the availability of both the physical and thermal habitats in the Anzac River, drone surveys were conducted biweekly at the reach-scale and once at the riverscape-scale. Surveys were conducted using a DJI Matrice 200 V2 quadcopter drone equipped with a Zenmuse XT2 four-band (one band each of red, blue, and green, and one band of forward-looking infrared/FLIR) imaging payload (Figure 4). Biweekly reach surveys were conducted

four times throughout the 2022 season on July 31, August 15, September 2, and September 15. The riverscape survey was conducted over three days between August 11-14. Surveys were conducted from a series of vantage points accessible through cutblocks along the Anzac River valley. River reaches within 3.3 km of each vantage point were mapped, which depending on the sinuosity of the survey section produced single-flight orthomosaics ranging from 2-14 Rkm in length. Surveys were flown as close as practicable to solar noon at which time the internal heterogeneity of thermal habitats within the wetted channel is the most exaggerated and visible to thermal sensors (T. Wilms, Nicola Valley Institute of Technology, *Personal Communications*).

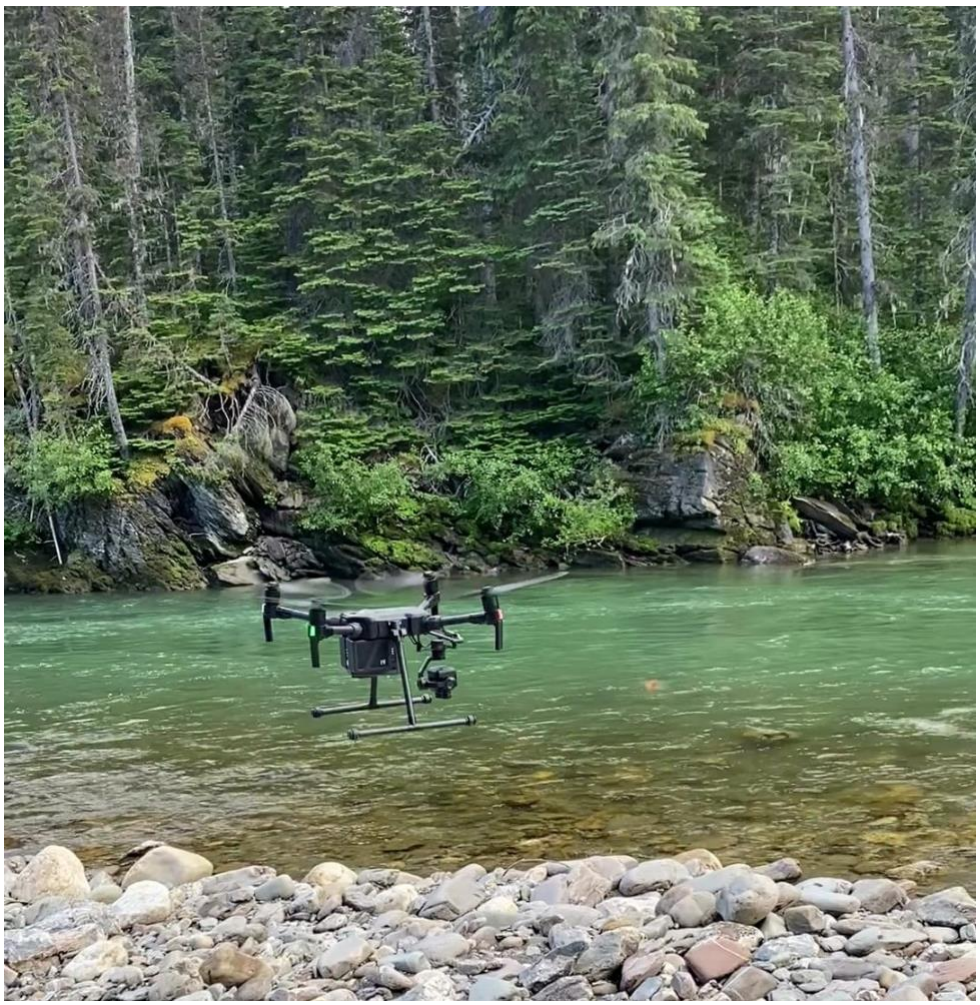

Figure 4. DJI Matrice 200 V2 quadcopter drone equipped with a Zenmuse XT2 RGB+FLIR camera on a downward facing (nadir) gimbal mount.

Thermal and physical images produced by the drone surveys were processed with Pix4Dmapper by Pix4D photogrammetry software (version 4.8.3; Educational License). Initial processing was completed separately for both the RGB and FLIR layers using the *Advanced Ag RGB* and *Advanced Thermal Camera* processing templates, respectively. Image pair matching was set to *Free Flight or Terrestrial*, and FLIR rasters and RGB orthomosaics export options were set to *merged GeoTIFF files*. All other point cloud processing, camera

configuration, and image georeferencing and datum selection options were left as *Automatic* and were derived from EXIF data stored in the raw drone image files.

Complementary to the 3-band colorized FLIR raster (which does not explicitly contain temperature data), an Index raster was produced by Pix4Dmapper which represents a single-band layer of radiometric temperature values across the pixels of the imagery. Subsequent cartographic tools used the FLIR raster, while temperature-related data analyses and visualizations used the values from the Index raster.

Minor spatial differences in the completed RGB and FLIR+Index rasters (derived from the different pixel widths and resolutions of the dual cameras aboard the imaging payload) were corrected by georeferencing the RGB layers to the FLIR layers using a spline transformation with at least 10 control points per layer in ArcGIS Pro (version 3.1.2; Advanced License through UNBC). By georeferencing the layers in this order (i.e., RGB to FLIR), the temperature pixel Index of the FLIR raster was preserved. RGB, FLIR, and Index layers were then imported into QGIS software (version 3.32.1; GNU General Public License) for further processing (Figure 5).

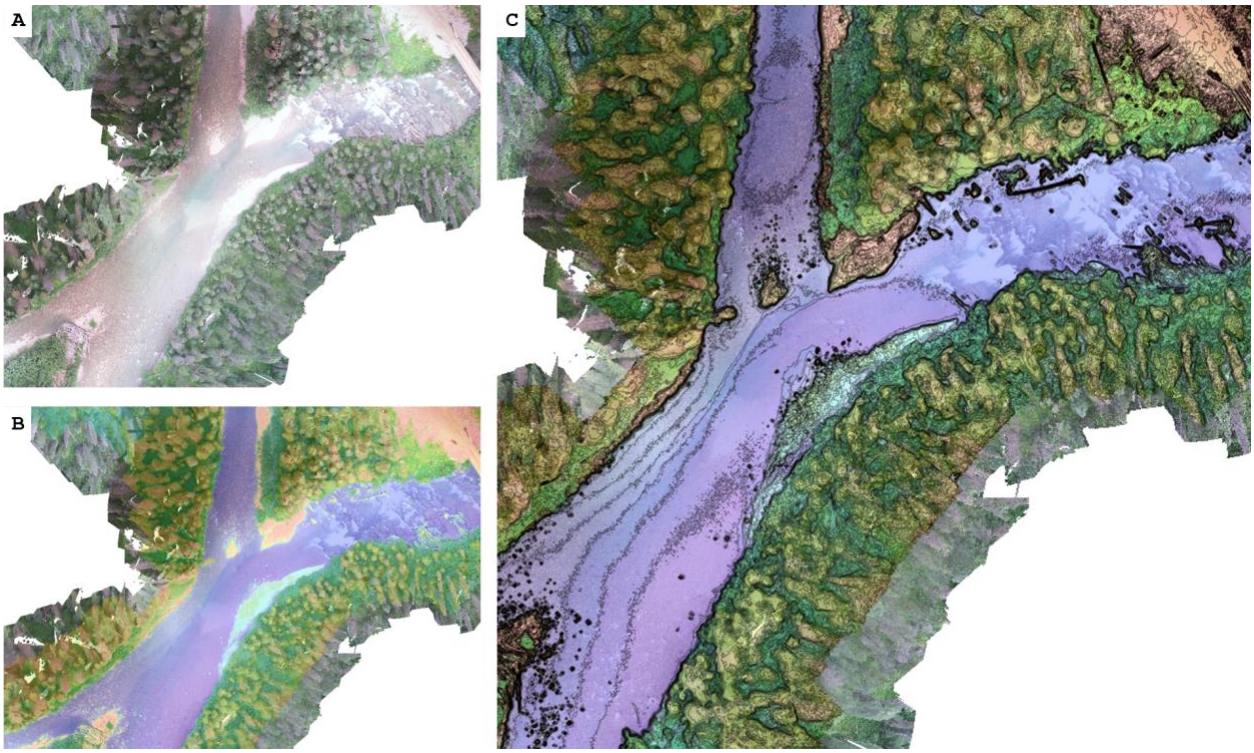

Figure 5. Drone surveys produced raster layers of RGB (panel A), FLIR (panel B), and temperature index rasters which were extracted by 0.25 °C isotherms to produce a composite image of the riverscape (panel C).

FLIR sensors are non-penetrating and thus produce only the skin temperatures of an object (in this case the surface of the Anzac River). To calibrate the temperatures of the Index raster used in reach-scale analyses, HOBO MX2201 temperature loggers were deployed with

a density of one every 100 m across each study reach. Calibration values for each Index layer were calculated as the mean pixel difference between the HOBO logger temperatures over the duration of the flight and the corresponding surface temperatures recorded by the FLIR sensor at each location. Calibration values were applied to each Index layer using the raster calculator.

As riverscape-scale imagery was collected across multiple days and as such was subject to spatially and temporally varying insolation, cloud cover, temperatures, and local effects, measured temperature values from riverscape FLIR indices were not directly comparable between sections, but rather represent local thermal distributions at the time of imaging. As such, riverscape FLIR index rasters were calibrated more coarsely than at the reach scale. For analyses into riverscape-scale habitat distributions, indices were used as a metric of the local thermal heterogeneity associated with habitat features and calibration of raw radiometric distributions to absolute temperatures was not necessary. For use in climate change warming analyses, stitched imagery from each flight was calibrated so that the median water temperature of each wetted channel was 14 °C. As variable local conditions across the survey dates and the scale of the Anzac River together preclude drone photogrammetry from being an effective tool for continuous mapping of absolute temperatures (which would require an extensive calibration array at the riverscape scale), this approach of calibrating riverscape indices was used to represent a snapshot of the extents of thermal habitats at a fixed point in the diel temperature cycle of each reach to compare the relative change in thermal habitat extents under various scenarios.

To define a range of available temperatures against which to compare thermal use data from the radio tagging study, spatial FLIR indices were interpolated across the four survey dates using a calibration value of hourly mean temperature values from the HOBO loggers and assembled as a gif using the R packages `terra` (Hijmans 2023) and `animation` (Xie 2013, 2021). An hourly metric of the spatial aggregation of temperature clusters from the interpolated rasters was computed using the R package `landscapemetrics` (Hesselbarth et al. 2019). Patchiness was calculated as:

$$PD = \frac{N}{A} * 10000 * 100 \text{ (Equation 1)}$$

where *PD* is the metric of patchiness which increases as the landscape becomes more patchy, *N* is the number of patches, and A is the wetted area of each reach (Hesselbarth et al. 2019). The metric of patchiness was further used in the radio telemetry study described below. Rasters from each survey date were calibrated to the duration of their corresponding snorkel swim and polygonised by 0.5 °C isotherms for use in data analysis for the snorkel study.

To extract only wetted pixels for use in data analyses, river masks were created by rendering contour lines from the Index layer and assembling a polygonised mask layer from isotherms selected at the land-water interface. Reach-scale drone surveys were clipped to the extent of the range of the radio telemetry receivers and were further subset into index reaches for the snorkel surveys. At the reach-scale only, a substrate layer of three polygon

classes (fines and small gravels, large gravels and cobbles, and bedrock and boulder gardens) and a habitat layer of four polygon classes (pools, riffles, runs, and rapids) were created manually by defining polygons for each habitat class over drone orthomosaic images.

Snorkel surveys

Snorkel surveys were conducted along a subset of each study reach on the same dates as the drone surveys (Figure 6) with two exceptions; the snorkel survey associated with the July 31 flight for reach A was conducted two days later on August 2 and no snorkel survey was conducted for the first date in reach B (this was due to time lost through a combination of drone repair logistics, a week of slow-moving Super-B convoys along access roads, and an inopportunely broken drysuit zipper at the time of the survey attempt).

Each study reach was broken into 100-m intervals (subreaches) over which all observable Arctic grayling and bull trout were counted, and mountain whitefish were noted on a presence/absence basis (due to their high abundance, it was not possible to reliably enumerate mountain whitefish). The surveys were conducted by two people swimming each subreach in succession and then comparing their counts; mean count values were used in analyses in cases where counts differed between swimmers. Where lanes were wide enough to support two swimmers side-by-side, swims were conducted concurrently and total counts were used. Snorkel counts and presence/absence data were integrated with their assigned polygon layers using the R package `sf` (Pebesma and Bivand 2023; Pebesma 2018) and then merged with reach-scale temperature, habitat, and substrate layers.

Figure 6. A snorkel survey in reach A.

Snorkel data were analyzed using Resource Selection Probability Functions (RSPFs) following an unmatched used-available design (Lele and Keim 2006). RSPFs are used to analyze animal locations through space and relate whether different habitat covariates are selected for disproportionately from other available habitat types. We apply RSPFs in this study to estimate selection using Arctic grayling locations in snorkel reaches and physical habitat parameters from the drone surveys. The RSPF takes the form:

$$w(x) = \exp(\beta_1 x_1 + \beta_2 x_2 + \cdots + \beta_k x_k) \quad \text{(Equation 2)}$$

where $w(x)$ is the predicted pixel probability of occurrence of the function and $\pm \beta_k x_k$ denotes preference or avoidance of each habitat covariate. Snorkel data were modeled as the probability of selection by Arctic grayling against temperature, habitat class, substrate class, and bull trout and mountain whitefish presence/absence covariates as well as bull trout and mountain whitefish interactions with habitat type. Eight RSPF models were fit and ranked with AIC using the R package `ResourceSelection` (Lele and Kiem 2019).

While snorkel data used in the RSPFs were reduced to binary used/available metrics, snorkel counts of Arctic grayling and bull trout were used in modeling changes in the efficiency of behavioral thermoregulation over time from the radio study data. While the proposed study intended to compare this metric for periods when bull trout were present to periods when they were presumed absent after a general migration date, bull trout persisted in some reaches late-season (see Results and Discussion). A metric of relative abundance of bull trout by study reach (BT_S) was created for the three periods bounded by the four snorkel surveys to be compared against Arctic grayling behavioral thermoregulation efficiency in the radio tagging study.

The riverscape drone survey produced a continuous map of the first 52 km of the Anzac River across 13 flights (Table *1*).

Table 1. Dates and times of the riverscape scale drone surveys.

Flight	Date	Start	Stop
1	2022-08-11	13:09	13:21
2	2022-08-11	13:38	13:50
3	2022-08-11	15:07	15:25
4	2022-08-12	10:38	10:53
5	2022-08-12	14:33	14:45
6	2022-08-12	16:04	16:12
7	2022-08-12	16:48	17:09
8	2022-08-14	10:49	11:02
9	2022-08-14	11:59	12:13
10	2022-08-14	12:49	12:58
11	2022-08-14	13:43	13:57
12	2022-08-14	14:40	14:55
13	2022-08-14	15:53	16:09

Riverscape orthomosaics were compiled into a single file to produce a continuous RGB + thermal map of the Anzac River over the 52 Rkm that were surveyed in this study. To expand the pool-centric results from the reach-scale study (see Results) to the context of the greater riverscape, the riverscape was surveyed for the distribution of pool habitats in QGIS software. Pools were identified as areas where the water deepened, and surface flow patterns showed evidence of slowing compared to adjacent flows. Pools typically formed in the corners of river bends, behind hydraulic features, at confluences, and at times where the river channel deepened and widened and midchannel flows changed. To create an index of pool quality which could be compared across the riverscape scale, individual pools were scored for size, internal thermal heterogeneity, effects of shade, and relative depth. Scoring criteria were defined as follows:

I. Size: A metric which considers channel width so that pools are weighted relative to their local availability in the riverscape. Five levels were defined, and examples of each size class are presented in Figure 7:
    a. Size 0: Very small, but larger than micropools which cannot be clearly identified at the imagery resolution. Possibly ephemeral features caused by temporary river features such as isolated logs or exposed large boulders creating collecting pools in their wake.
    b. Size 1: Small pools taking up a relatively small proportion of the overall reach width (<25%) and were approximately equal in length and width.
    c. Size 2: Pools which took up a large proportion of the overall reach width (25 - 100%) but were less than two reach widths in length and/or contained inclusions of other habitat types.
    d. Size 3: Large pools which took up the entire width of the reach and had a length of two reach widths or more.
    e. Size 4: Notably large pools or pool complexes which dominate the river in each reach.

II. Shade: When pool isotherms were under shadow from surface features or isolated cloud cover, a binary 1/0 metric was indicated to compensate pool scoring for the effects of shade muting thermal signatures in the imagery (Figure 8).

III. Deep: A binary metric indicating when a pool's depth is significant relative to the surrounding river suggesting that there is likely greater internal heterogeneity than was captured by thermal signatures at the surface. Defined when the bottom of the pool was not visible in well-lit imagery and when large plunge features created surface disturbances over deep plunge pools.

IV. Isotherm: A count metric determined by the number of isotherms from the center of the pool's thermal signature to the unconfined edge of the pool. Negative values were assigned if the pool's thermal centroid was warmer than the ambient river (Figure 9)

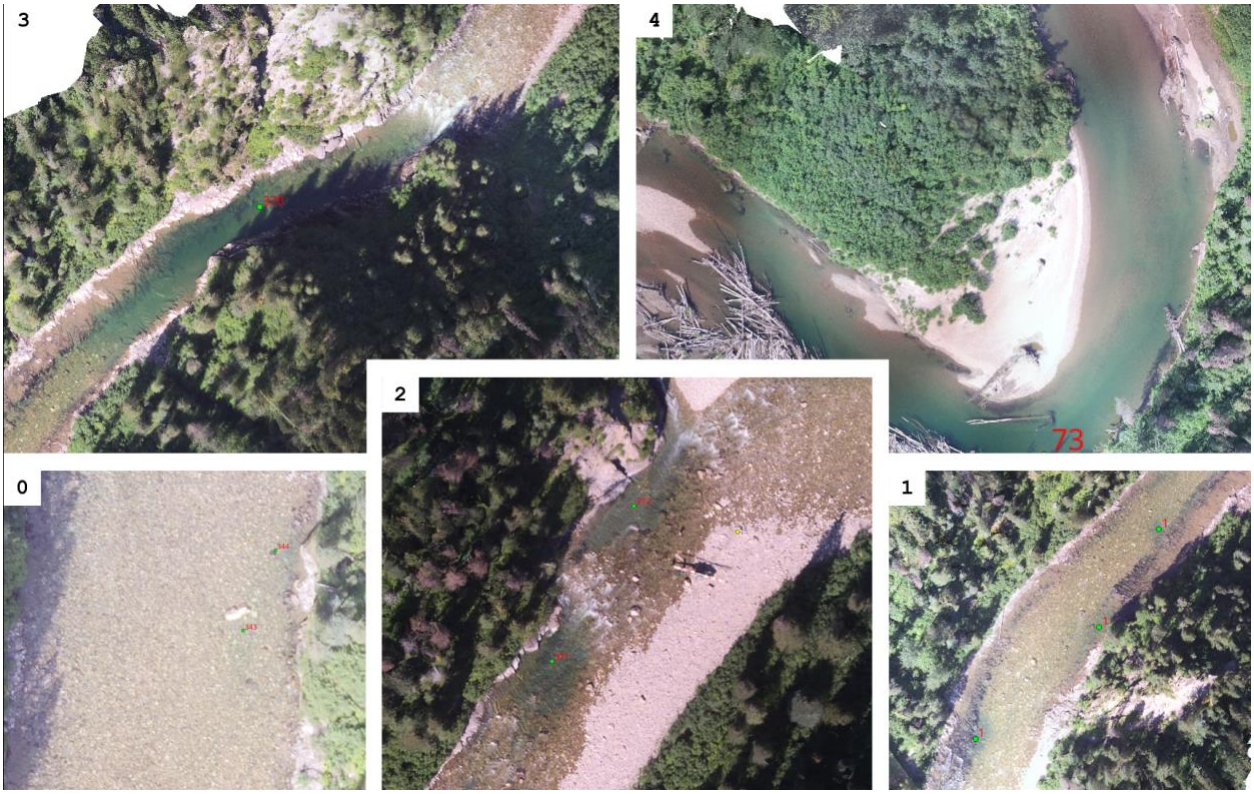

Figure 7. Example pools from the five ranked size classes. Panel numbers indicate pool size.

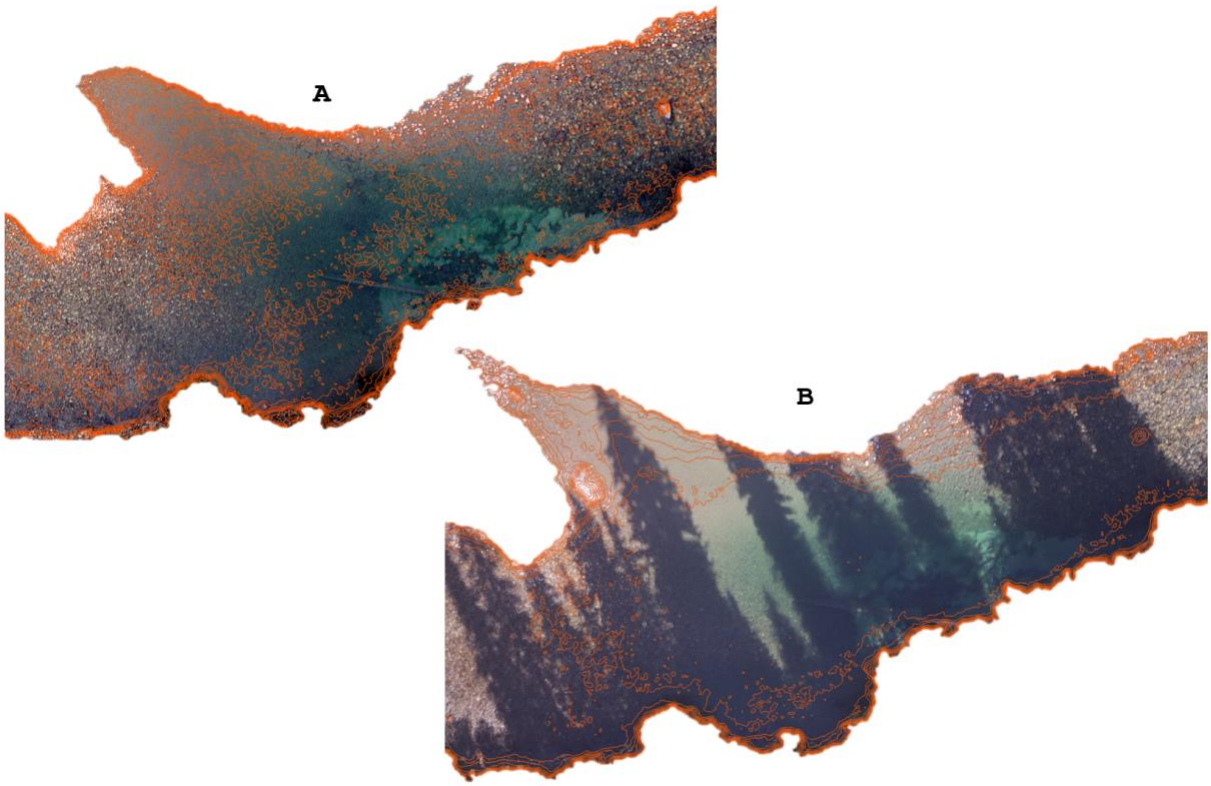

Figure 8. Thermal signatures visible in well-lit pools (A) can become muted when cast in shadow (B).

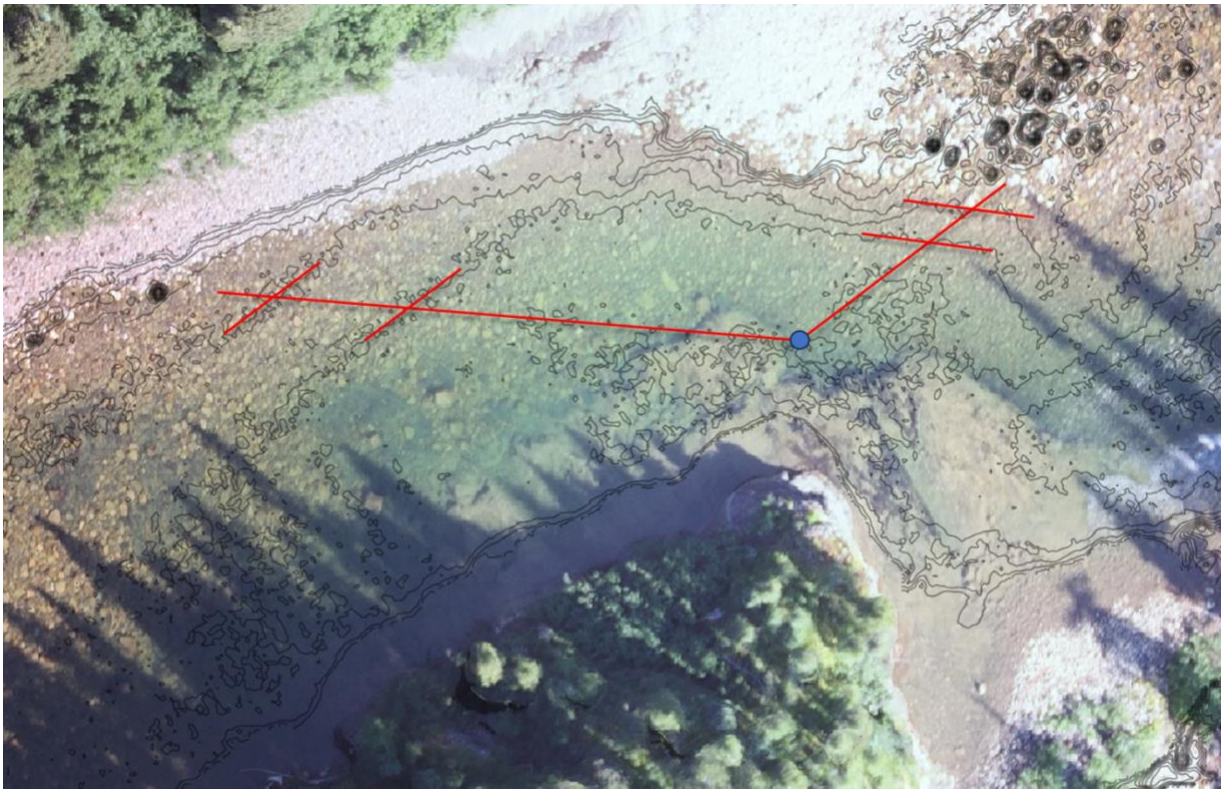

Figure 9. Isotherms were counted as the number of complete isotherms between the centroid of a pools thermal signature to the unconfined edge of the pool. This is an example of a pool with two isotherms.

Scored pools were aggregated by Rkm and the mean pool score in each Rkm was used as a metric of pool quality in each reach across the river. To ensure comparability with other FWCP-funded investigations in the region, Rkm start-stop waypoints were used from data provided by John Hagen and Associates (2023, *Personal Communications*). To highlight areas which may be of high conservation potential, pool scores were plotted by latitudinal river distance at different levels of aggregation (individual pools and 1, 5, and 10 Rkm aggregations), and spatially visualized at the 1 Rkm scale across the riverscape.

Riverscape-scale snorkel data was provided by collaborators John Hagen and Associates and the methods described in their report (Hagen and Stamford 2023; PEA-F23-F-3631). Population estimates at each reach defined in their N-mixture model were regressed against Rkm scores. Regression outputs were used as a general predictor of potential Arctic grayling population densities in each Rkm.

Rasters for climate change forecasting were created by tuning the riverscape index raster to various downscaled climate change scenarios (half-degree steps of 0, 0.5, 1.0, and 1.5, °C over 50 years to the 1.5 °C post-industrial warming scenario defined by the Intergovernmental Panel on Climate Change (IPCC)). A metric comparing the extent of habitats that fell within the thermal preference range (T_{SET}) as defined by the shuttlebox study was defined to predict the extent of thermal habitat restriction across each scenario.

Shuttlebox experiments

Shuttlebox studies are controlled, laboratory-based experimental approaches for establishing a range of environmental preferences for an individual (Christensen et al. 2021). Shuttlebox experiments were used in this study to determine a range of thermal preferences for adult Arctic grayling during their summer feeding migration. These data were used as metrics against which to compare *in situ* thermal habitat use data collected by the radio tagging component of the study. A total of 17 fish were used in shuttlebox experiments; ten in successful thermal preference experiments, ten in successful heat transfer experiments (with seven of these individuals also used in the thermal preference experiments), and three in experiments which were discarded. Thermal preference experiments were conducted between August 28 and September 10, 2022.

The shuttlebox field laboratory was deployed at Goose Lake Recreation Site near the confluence of the Anzac and Parsnip Rivers (Figure 10). Data acquisition systems were powered by a parallel circuit of generators which allowed for lossless power during refuelling cycles over each 24-hour experiment. Operations of the field laboratory and power supply were authorized by RSTBC under Section 16 of the Forest Recreation Regulation (File: 16660-21-01- REC 1141; K. Mohr, RSTBC, *Personal Communications*).

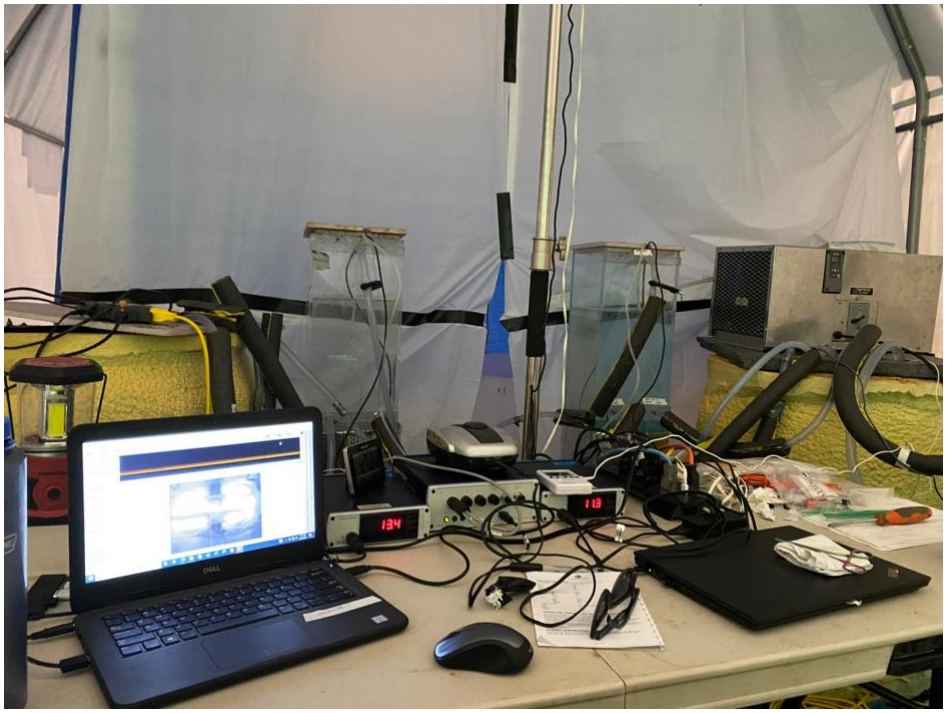

Figure 10. The shuttlebox control system with temperature regulator units, heating and cooling baths, and buffering tanks.

The shuttlebox itself consisted of two 1-m diameter round tanks which were randomly assigned as either the warming tank or the cooling tank at the start of each experiment. The tanks were connected via a 20 cm passage chamber which allowed individuals free-

choice movement between the two thermal environments (Figure 11). Temperatures in each tank were initially defined and dynamically controlled by Shuttlesoft software (Loligo Systems) via an actuated system of cameras, thermometers, water pumps, hoses, coils, and external heating and cooling baths.

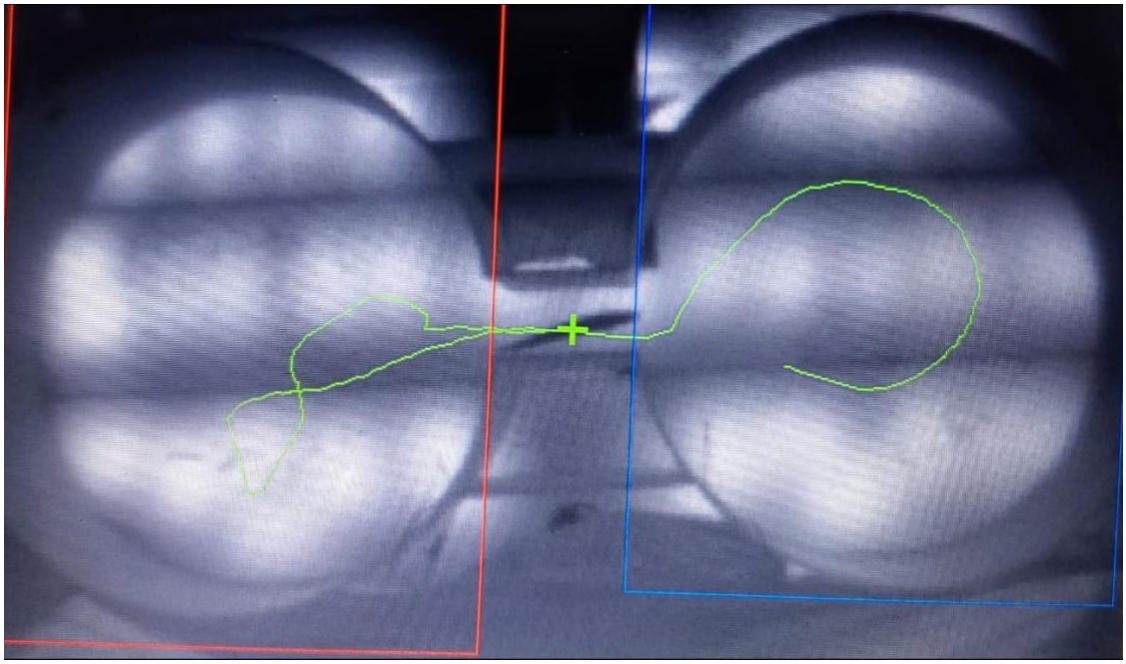

Figure 11. A still from the Loligo Shuttlesoft software (viewed from above) monitoring an Arctic grayling as it shuttles between tanks. The green line represents the track of the Arctic grayling over the last 30 seconds.

Water used in the shuttlebox system was transported by truck from the Anzac River, which allowed all Arctic grayling captured for this study to be released back into the river at the end of each experiment. At the start of each experiment, shuttlebox temperatures were set to ± 1°C from ambient river temperature at the time and location of capture in the warming and cooling tanks, respectively. Arctic grayling were captured and transported to the field laboratory site in an aerated cooler, sampled for sex, length, weight, and dorsal fin length and randomly assigned to a starting tank.

During each experiment, Shuttlesoft monitored fish positions within the tanks using an overhead camera against UV underlighting beneath the shuttlebox. Indicated by whether the fish was in the warming tank or the cooling tank, the system warmed or cooled both tanks at a max rate of 2°C/hour. Each time the fish "shuttled", or moved between the tanks, the heating or cooling process would reverse directions. In a controlled shuttlebox setting in which the effects of predators, prey, diel, forage availability, etc. are removed, these movements enable fish to regulate body temperature so that it remains within a preferred range.

Data from the first four hours of each experiment were removed as an acclimation period while the individual explored and learned the shuttlebox environment. The remaining 20 hours of continuous temperature data were subset into the 25th, 50th, and 75th quantiles. For

each individual, thermal preference T_{PREF} was defined as the 50th quantile of occupied temperatures and the preferred temperature range T_{SET} was defined as between the 25th and 75th quantiles. The preferred temperature range T_{SET} was then used in the analysis of behavioral thermoregulation from the radio telemetry study.

Heat transfer coefficient k

The shuttlebox system was also used as a controlled environment to conduct a second set of experiments to determine a heat transfer coefficient *k* for adult Arctic grayling. Coefficient *k* is a metric measuring the instantaneous rate of change in body temperature based on the difference between body temperature T_B and the ambient water temperature T_A (Pépino et al. 2015). Based on Newton's law of cooling, coefficient *k* is used in this study to convert temperature data from the externally mounted radio tags to the physiologically-relevant interior body temperatures of the fish.

Adult Arctic grayling used in the heat transfer trials were tagged both internally and externally with synchronized temperature loggers (Star ODDI DST Nano-T) which monitored both ambient and body temperatures at 5-second intervals over each 3 hr. and 45 min. trial. Internal tags were inserted esophageally using a plastic applicator coated in Vaseline and removed after the experiment. External tags were temporarily mounted close to the body (under the dorsal fin) on an anchor tag (FLOY Mfg. T-Bar Anchor). The anchor tag remained on the fish after the experiment for further mark-resight work (Figure 12).

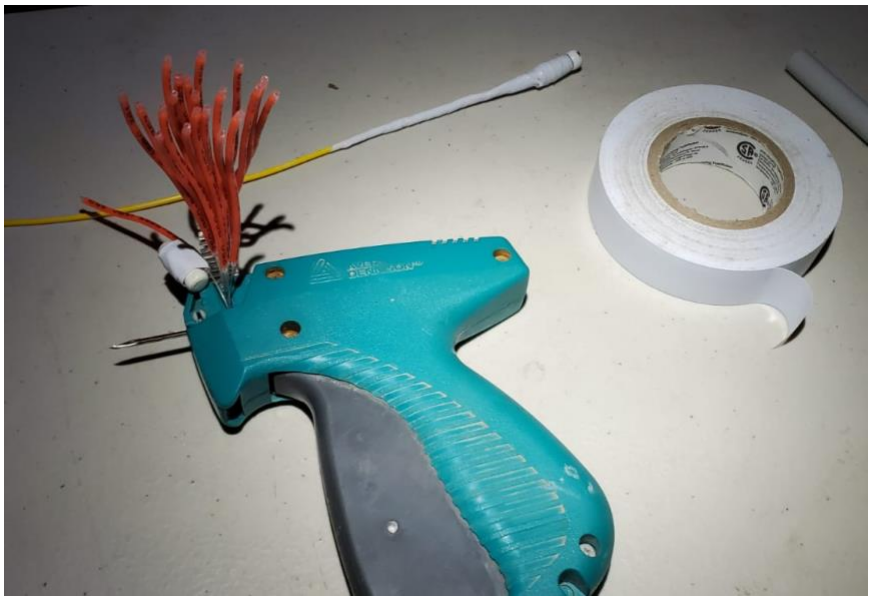

Figure 12. A pair of synchronized Star ODDI DST Nano-T loggers prepared for internal and external application.

In comparison to the *dynamic* shuttlebox experiment described above, heat transfer experiments used Shuttlesoft's *static* mode in which the temperature of each shuttlebox tank was manually set and maintained by the user. This allowed for an experimental design which consisted of five consecutive trials in which each fish would be exposed to a pre-defined shift in temperature and then monitored for 45 minutes while body and ambient

temperatures converged. Temperature shifts were defined as a set of decreasing temperature differentials starting at a 2 °C interval of ± 1 °C from ambient river temperature at the time of capture and narrowing by 0.5 °C per step. The direction of each temperature shift was reversed from the previous trial (i.e., cooling trials were immediately followed by warming trials) and initial direction was determined by a randomized starting tank for each fish. The heat transfer experiments were conducted immediately following the shuttlebox trials for seven of the ten fish sampled; three additional experiments were done using purpose-caught fish. Heat transfer experiments were conducted after the thermal preference experiments rather than concurrently with them as it was observed during early experiments (data not used) that the Star ODDI tags affected behavior in the shuttlebox (e.g. fish would stop exploring the tanks or try to remove the esophageal tag using the corner of the shuttlebox tanks and the passage, confounding any results which assume behavior is based on choice among available thermal environments alone).

Data from the heat transfer experiments were used to estimate a heat transfer coefficient k using non-linear mixed effects models. The heat transfer equation was:

$$T_{B_t} = T_A + \left(T_{B_{t-1}} - T_{A_t}\right)e^{-kt} \text{ (Equation 3)}$$

where T_A is the ambient temperature (external tag) and T_B is the body temperature (internal tag) at each five second interval t. Two covariates, centered body weight (W_C) and a 2-level factor indicating a warming or cooling trend (*trend*), were used as predictors (fixed effects) of k and fish ID was used to as a random effect on the model intercept (Pépino et al. 2015). A total of 4 candidate models containing different combinations of predictors and a null model on the intercept were fit with maximum likelihood methods and the top models selected by AIC were refit using maximum restricted log-likelihood in the R package `nlme` (Pinheiro and Bates 2022). The top model selected by AIC was then reevaluated using different autocorrelation structures and the final model was fit using a first order autocorrelation structure. The estimated value of coefficient k from the top model was later used to convert radio tag temperatures to body temperatures.

Biologging with radio telemetry

Between the two study reaches, 50 adult Arctic grayling were captured and tagged with temperature and activity sensing radio transmitters (model MCFT-3, Lotek Wireless). Considering many aspects of this study are explicitly spatial, it is important to note here that the radio telemetry tags and receivers used in this study were set up for biologging data, not triangulating fish positions. Radio tags were affixed to the dorsal surface using an interrupted suture technique following the methods in (Crook 2004) using monofilament suture line to allow the tag to detach naturally after some time (Figure 13). Tagging was done in accordance with protocol (# 2021-05) approved by the University of Northern British Columbia's Animal Care and Use Committee. All Arctic grayling examined across all stages of this project were captured on barbless dry flies and tagged on-site.

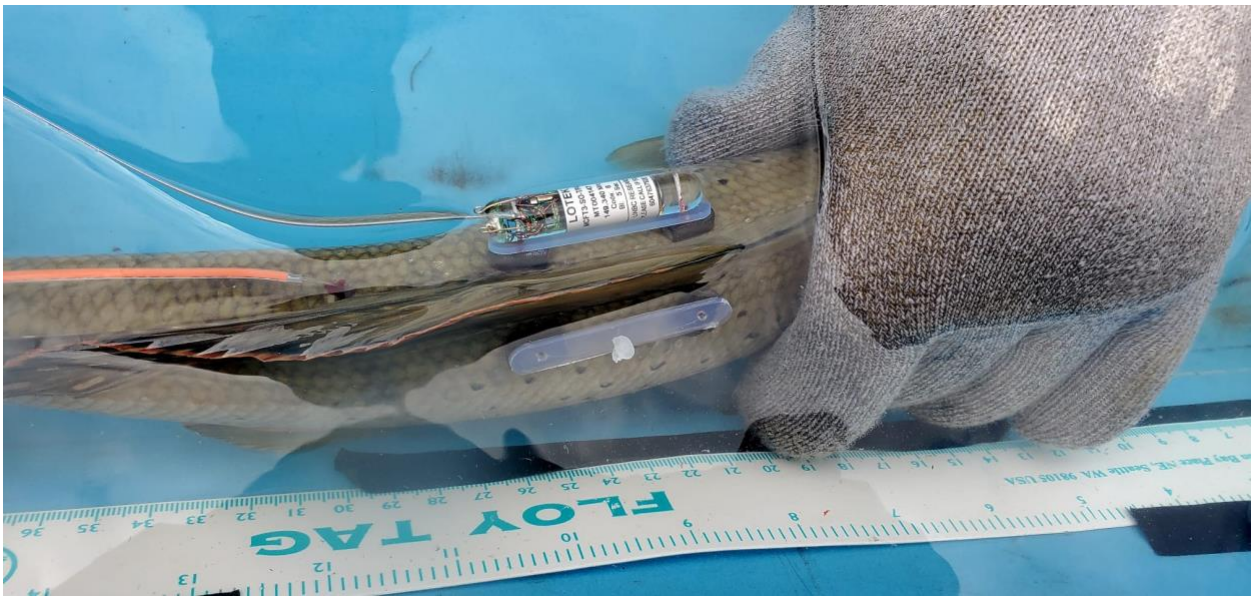

Figure 13. A Lotek MCFT-3 radio tag mounted using interrupted sutures to the dorsal surface of an Arctic grayling.

To monitor the deployed radio tags, an array of solar-powered radio receivers were installed along each study reach at vantage points on top of bluffs and cliffs providing maximum line-of-sight coverage for receiver antennae (Figure 14). To protect against potential data loss, receiver stations were downloaded periodically throughout the field season. Data recorded by the radio tags were indexed by study hour with hour zero starting at 2022-07-31 00:00:00 PDT and hour 1,120 ending after 2022-09-15 16:00 PDT. The tags transmitted measurements of both temperature and activity twice per minute whenever they were in range of the receiver array.

Figure 14. Radio receivers were set up at vantage points along each study reach.

Raw temperature data from the radio tags were exceptionally noisy (containing frequent outliers and measured values of water temperature that exceeded air temperatures) and were pre-processed for an underlying signal using a two-pass filter. The first pass removed low power detections (RSSI < 100), false tag ID signals, and sequential external temperature detections which deviated more than ± 2 °C between a maximum of 30-minute steps. The second pass applied a fine-tuning filter which refined each tag's data based on three factors: (1) initial tagging date which removed detections before one hour post-tagging which both removed occasional false detection points from before tagging and allowed body and ambient temperatures to reconverge after capture; the distribution of both body and ambient temperatures which removed data points which were beyond what ambient temperatures would suggest were possible, and evidence of mortality or emigration from the study reach (emigration was determined as cases when a clear radio signal degraded to sporadic points with long times between them indicating the tag had moved to or beyond the periphery of the radio receivers' detection range or had become

otherwise obscured). Fine-pass filters were made based on inspection of individual hourly temperature plots. Summarizing all detections by hour across the study period had a smoothing effect on the data, and unrealistic outliers and changes in behavior were able to be more easily identified and removed. The application of a combined coarse and fine filter was able to successfully clean the bulk of the data.

External radio tag data were converted to internal body temperatures (T_B) using the heat transfer coefficient k derived from the shuttlebox experiments as described above. Initial T_B was defined for each tag as a random draw from a uniform distribution of ± 1 °C from the first radio tag temperature detection and T_B was estimated recursively with the heat transfer formula (Equation 2). Hourly values of T_B were defined as the median of the temperatures experienced each hour.

Hourly metrics of individual deviation of both T_B and T_A from the T_{SET} range (from the shuttlebox study) were computed as d_B and d_A, respectively. These metrics represent both the accuracy of Arctic grayling body temperature regulation (d_B) and the quality of available thermal habitats (d_A) with respect to T_{SET} through time (Blouin-Demers and Weatherhead 2001). From these, an hourly index E was calculated which represents the effectiveness of behavioral thermoregulation through time, with values close to zero indicating poor effectiveness (thermoconformity) and values close to one indicating efficient thermoregulatory behavior. Index E is computed as:

$$E = 1 - \left(\frac{\overline{d_B}}{\overline{d_A}}\right) \text{ (Equation 4)}$$

where the overbars indicate mean hourly values in deviation metrics (Blouin-Demers and Weatherhead 2001). A further metric, E_X, was computed which represents the extent to which Arctic grayling exploited their thermal range T_{SET} on days when it was available in the environment. E_X was calculated as the percentage of time each tagged Arctic grayling spent within its T_{SET} range when it was available in their environment (i.e., when d_A = 0; Blouin-Demers and Weatherhead 2001; Christian and Weavers 1996).

The activity metric transmitted by the radio tags represents Vectorial Dynamic Body Acceleration (*VeDBA*), the vectorial sum of a tri-axial accelerometer in the tags (Qasem et al., 2012). Unlike temperature, an autocorrelative filter is not appropriate for cleaning acceleration data as fish can stop or start burst movements in an instant. *VeDBA* sensor values were filtered for noise by removing detections with low power (RSSI < 115) and those without corresponding hourly temperature summaries against which to regress. Hourly summaries for *VeDBA* were calculated as the maximum acceleration in each hour, as using the mean or median would produce an index mostly close to zero due to Arctic grayling behaviors during feeding in which they hold their positions in their current and forage using short burst movements.

Hourly values of index E were analyzed with a generalized additive mixed model as a function of mean water temperature, activity (*VeDBA*), thermal habitat patchiness, diel period, and body condition as described by the following equation:

$$y_{ij} = \alpha + \gamma_i + f\left(x_{mT,j}\right) + f\left(x_{patchinessT,j}\right) + f\left(x_{bc,i}\right) + f(x_{BT}) + f\left(x_{VeDBA,ij}\right) + \beta_1 x_{diel,j} + \varepsilon_{ij}$$
(Eq. 5)

where $y_{ij}$is the response (E) for individual i at time j; α is the intercept; γ_i is the random effect of individual on the intercept; $f(.)$ denotes smoothing functions of mean (mT) and a metric of temperature aggregations ($patchinessT$) at time j; body condition (bc) of individual i; relative bull trout abundance (BT); and maximum VeDBA exhibited by individual i at time j. β_1 is the effect of diel period (night, with day represented by the intercept) associated with time j; and ε_{ij} is the residual term. Both γ_i and ε_{ij} are assumed to follow a normal distribution with mean zero and standard deviation σ_γ and σ_ε, respectively. A total of 24 candidate GAMMs were fit modeling the logit response of Index E against the suite of covariates listed above which may influence the efficiency of behavioral thermoregulation.

5. Results and Outcomes

Drone and snorkel surveys

Biweekly drone surveys produced eight GIS layers; four each across the survey dates in both reaches A and B. Over the four survey dates (Table 2) in reach A, wetted width remained approximately the same, though water levels fluctuated. Beginning in the August 15 imagery and becoming most pronounced on September 2 baseflows before autumn rainfalls began, gravel bars begin emerging in the middle and lower portions of the reach, the lower of which persisted even after rainfall boosted water levels in the late season (Figure 15).

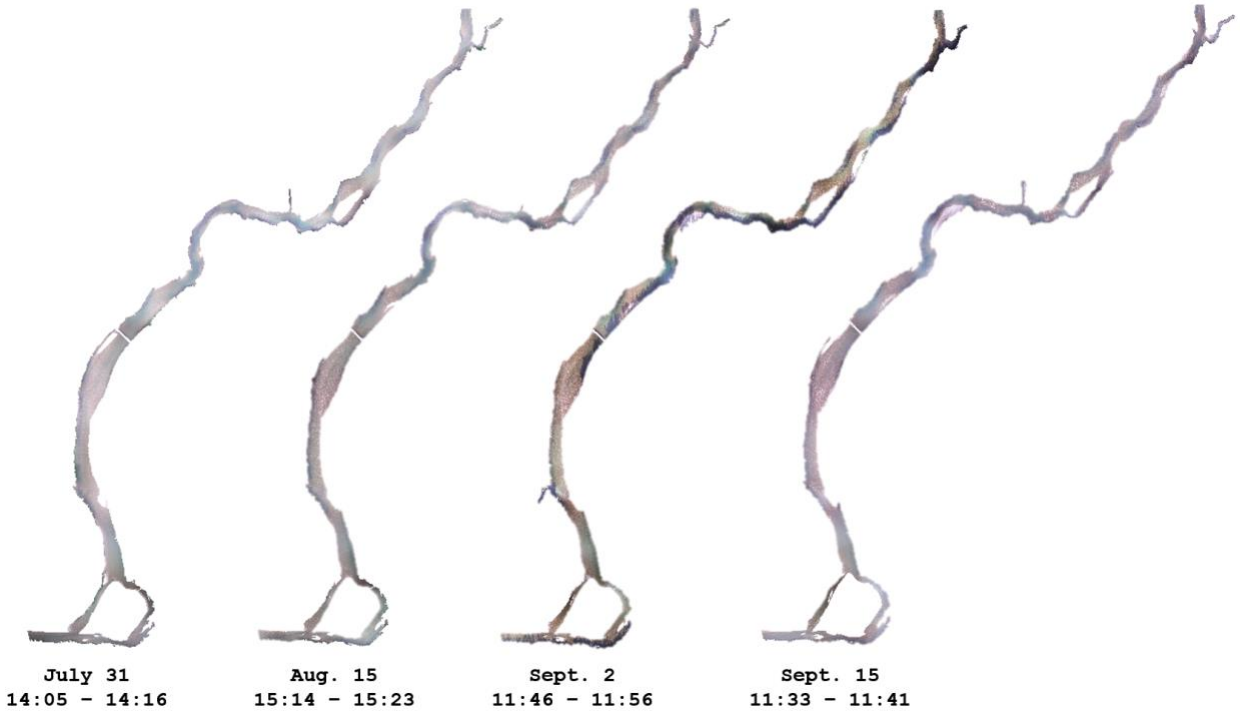

Figure 15. Survey images from reach A across the four survey dates. Flow direction in reach A is from top (northeast) to bottom (southwest).

Over the four surveys in reach B, channel width constriction to dropping water levels was slightly more apparent, but still not largely impacted. Vertical water levels impacted clarity more prominently between images in reach B than in reach A. As water levels dropped in reach B, an ephemeral side channel in the middle of the reach dried up and did not return after the July 31 survey (Figure 16).

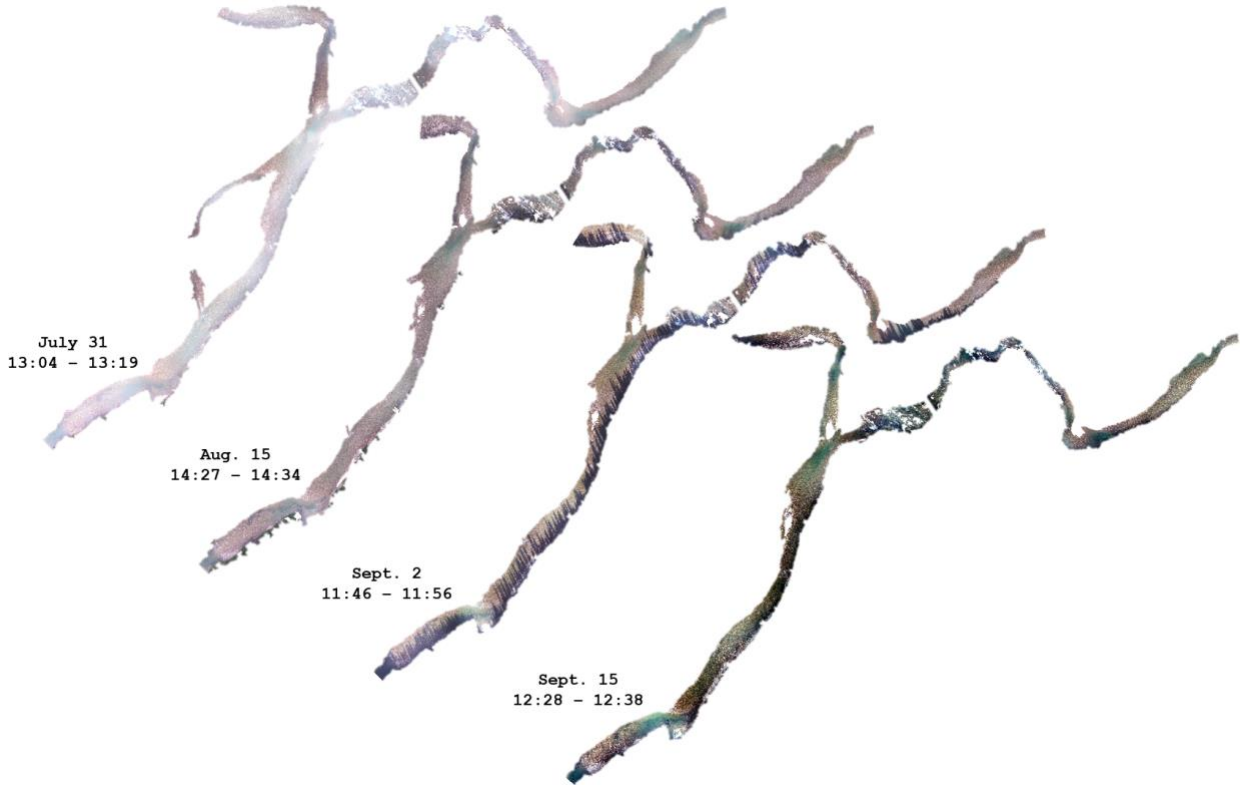

Figure 16. Survey images from reach B across the four survey dates. Flow direction in Reach B is top (northeast) to bottom (southwest).

An animation of spatial temperature indices by hour is available in Supplemental Materials (Figure 17; animations available online for reach A and reach B). Daily temperature patterns in reach A showed warming first in the exposed central reaches near the small warm tributary confluence while the middle reaches downstream of the bridge stayed cooler for longer into the morning. A mixture of warm and cool temperatures was readily available at the diel scale, with incursions of warm water happening in patches during diel thermal maximums until mid-August. In mid to late August, the entire reach was exposed to warmer temperatures daily, though patches of cooler habitat persisted at night. Temperatures began to cool in late August with a few flashes of warm water passing through until September 4, at which point a noticeable cool flash occurs and waters do not warm significantly again for the remainder of the sampling season. Throughout all four sampling dates, a patch of cooler shallow water persisted in the lower reach. Patterns in reach B were similar, with patterns of warm water restricting cool habitats to prominent pools occurring earlier in the season than in reach A (beginning on August 9 compared to August 15). While temperature extremes were more prominent in reach B, the total preclusion of any cool habitats only occurred during the hottest days of late August. Reach B followed a similar pattern to reach A in the late season, with a firm cooling switch happening after September 4.

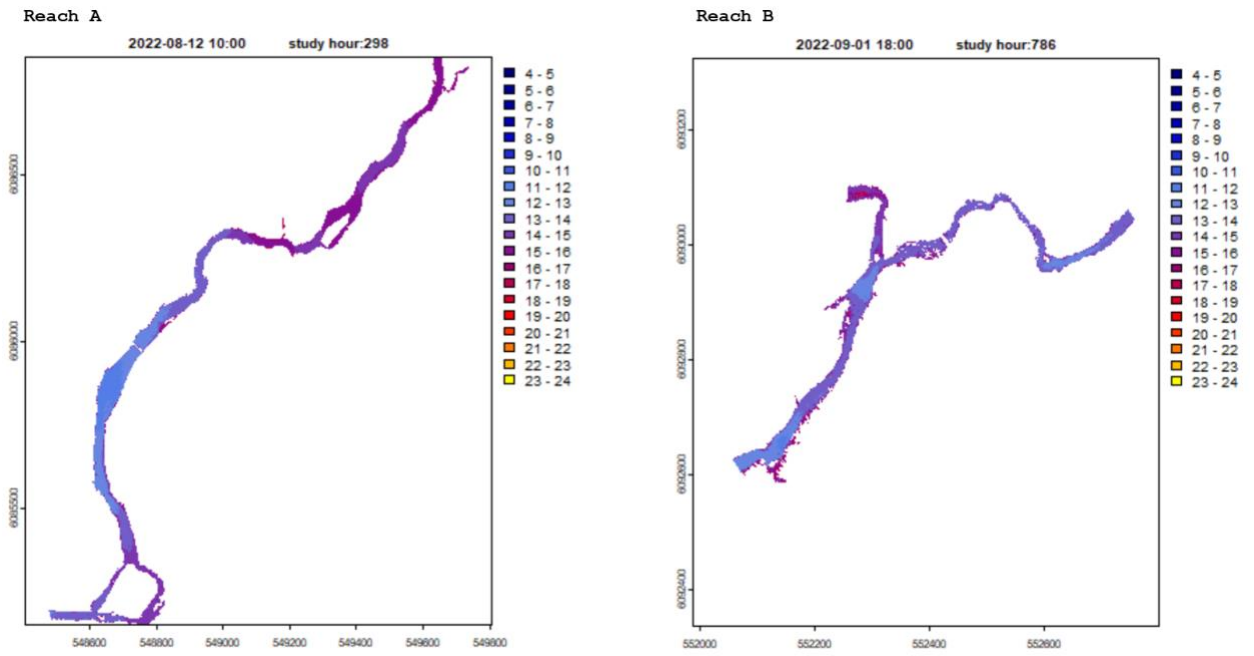

Figure 17. Stills from animated GIFs of spatial temperature distributions by hour across the study period. Animations available online: Link to reach A, Link to reach B

Table 2. Dates and times of each drone and snorkel survey and the temperature correction used to account for the difference in survey times.

Survey	Reach	Flight time	Snorkel time	Flight temp	Snorkel temp	Calibration diff
1	A	2022-07-31 14:05 - 14:16	2022-08-02 11:00 - 12:30	14.9	12.3	-2.6
1	B	2022-07-31 13:04 - 13:19	No snorkel survey	14.9	-	-
2	A	2022-08-15 15:14 - 15:23	2022-08-15 12:00 - 13:05	14.7	13	-1.7
2	B	2022-08-15 14:27 - 14:34	2022-08-15 15:10 - 16:00	15.9	16	0.1
3	A	2022-09-02 12:36 - 12:44	2022-09-02 13:30 - 14:20	11.4	12.1	0.7
3	B	2022-09-02 11:46 - 11:56	2022-09-02 15:00 - 15:55	11.2	14.4	3.2
4	A	2022-09-15 11:33 - 11:41	2022-09-15 14:45 - 15:33	9.9	9.8	-0.1
4	B	2022-09-15 12:28 - 12:38	2022-09-15 13:05 - 14:00	9.7	9.7	0

Counts of Arctic grayling, bull trout, and mountain whitefish organized by reach, subreach, and survey date are available in Table 3 and Table 4. Arctic grayling counts in reach A were the highest during survey A1 on August 2, dropping from 50 to 15 by the second survey. As the season progressed, numbers trended back upwards in reach A with 34 and 40 Arctic grayling counted on September 2 and 15. While there was no snorkel survey in reach B on the first survey date, the reverse trend was generally true; snorkel counts of Arctic grayling were the highest during the second survey on August 15, with numbers decreasing as the season progressed. These inverse trends suggest we may have captured the tail end of the upriver summer migration in early August (with fish moving from reach A towards reach B) and the beginning of the fall migration back towards overwintering habitats in the Parsnip River mainstem and lower Anzac River. Fish in both reaches were persistently

present in a few key subreaches; AR04 and AR07 (Figure 18)in reach A and BR01, BR03, and BR06 in reach B (Figure 19). All these subreaches were associated with pool habitats.

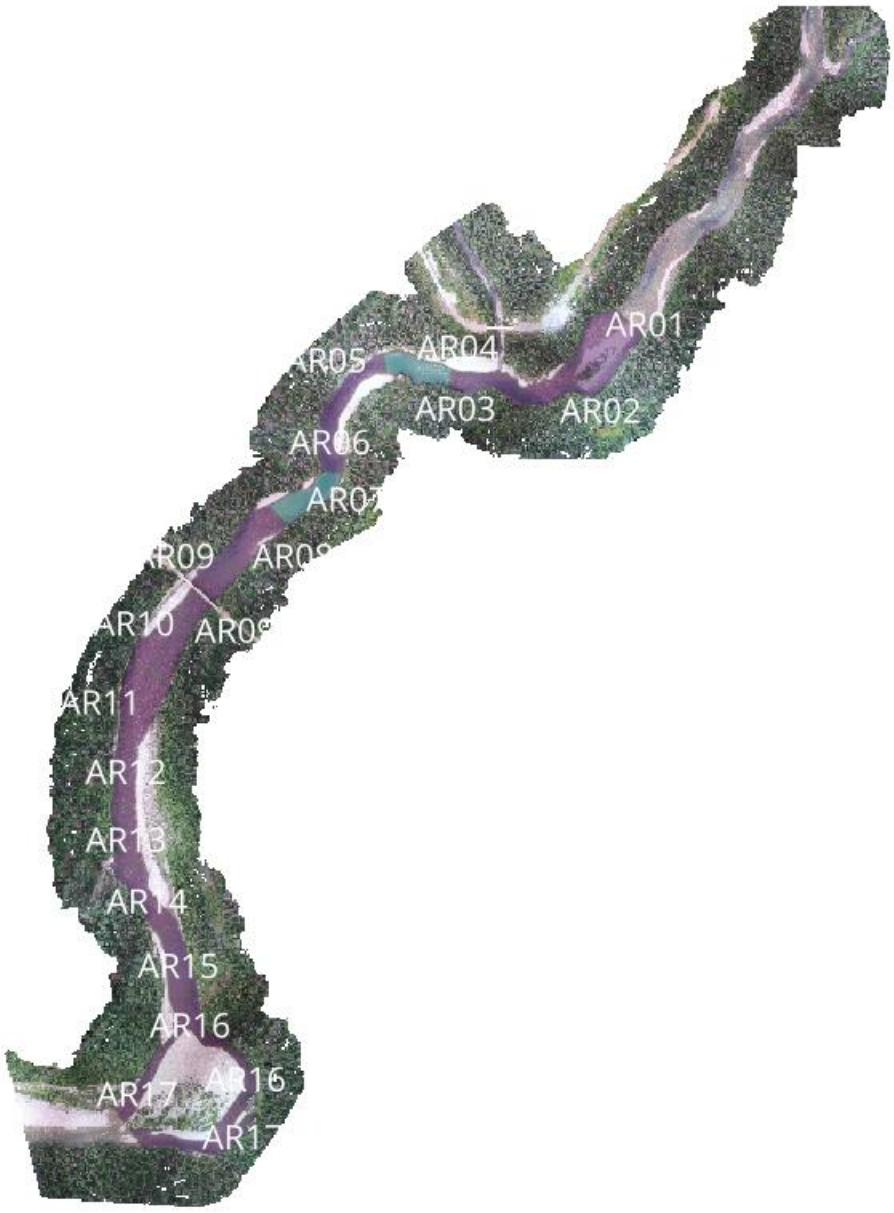

Figure 18. Snorkel subreaches in Reach A. Blue areas represent habitat where Arctic grayling were present across all four snorkel surveys.

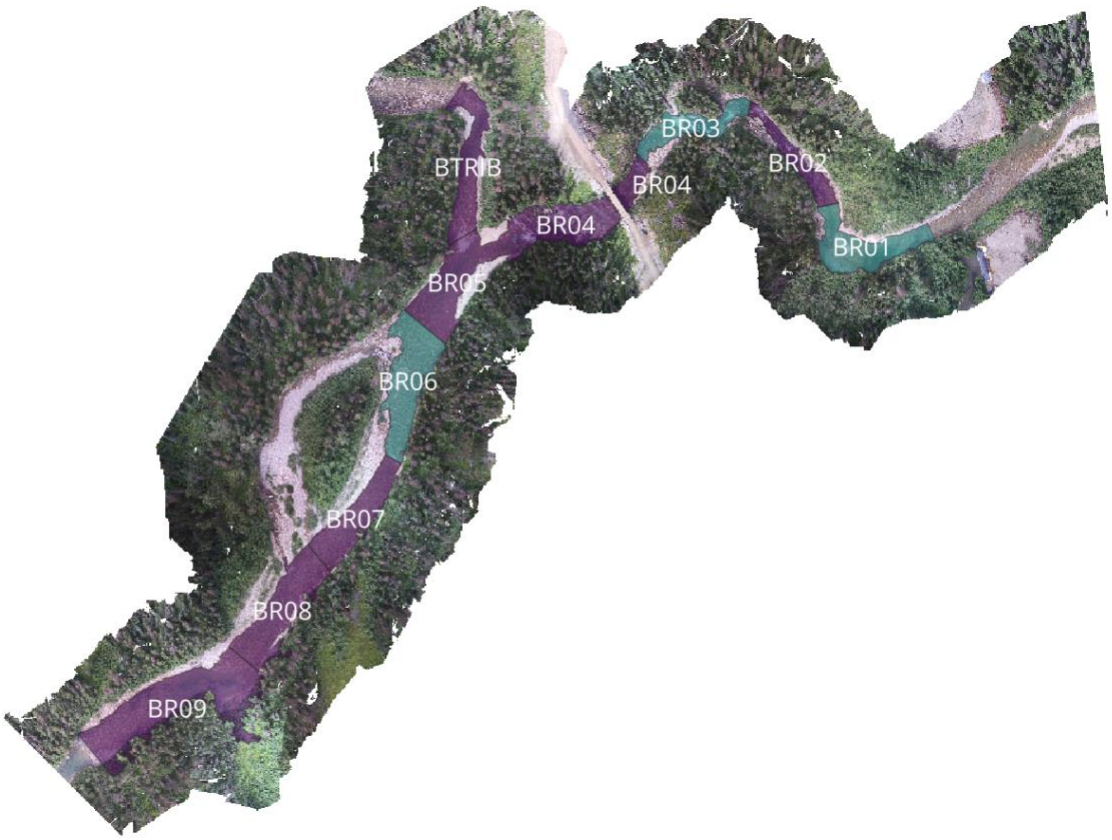

*Figure 19. Snorkel subreaches in Reach **B**. Blue areas represent habitat where Arctic grayling were present across all three snorkel surveys.*

Table 3. Snorkel survey counts of Arctic grayling, bull trout, and mountain whitefish presence in reach A.

Survey	Spp.	AR01	AR02	AR03	AR04	AR05	AR06	AR07	AR08	AR09	AR10	AR11	AR12	AR13	AR14	AR15	AR16	AR17
A1 (Aug. 2)	GR	7	18	3	1	14	0	5	0	0	0	0	0	0	0	2	0	0
	BT	2	2	1	1	0	0	1	0	0	0	0	0	0	0	0	0	3
	MW	0	1	1	1	0	0	1	1	0	0	0	0	0	0	0	0	0
A2 (Aug. 15)	GR	7	1	0	2	0	1	1	2	0	0	0	0	0	0	1	0	0
	BT	0	1	0	1	0	1	4	3	0	0	0	0	0	0	0	0	0
	MW	0	1	1	1	0	0	1	1	0	0	0	0	0	0	0	0	0
A3 (Sep. 2)	GR	7	3	7	4	0	4	3	0	5	0	0	0	0	1	0	0	0
	BT	0	0	5	2	0	0	0	0	0	0	0	0	0	0	0	0	0
	MW	0	0	1	1	0	0	0	1	0	0	0	0	0	0	0	0	0
A4 (Sep. 15)	GR	0	13	2	4	0	15	2	0	4	0	0	0	0	0	0	0	0
	BT	1	0	0	0	0	0	1	0	0	0	0	0	0	0	0	0	0
	MW	0	0	1	0	0	0	1	1	0	0	0	0	0	0	0	0	0

Table 4. Snorkel survey counts of Arctic grayling, bull trout, and mountain whitefish presence in reach B.

Survey	Spp.	BR01	BR02	BR03	BR04	BR05	BR06	BR07	BR08	BR09	BTRIB
B2 (Aug. 15)	GR	3	0	47	9	32	0	0	0	44	3
	BT	0	0	0	0	0	0	0	0	0	0
	MW	0	0	1	0	0	0	0	0	0	0
B3 (Sep. 2)	GR	6	0	10	0	0	0	0	0	15	0
	BT	0	0	2	0	0	0	0	0	0	0
	MW	0	0	1	0	0	0	0	0	1	0
B4 (Sep. 15)	GR	2	0	2	0	6	0	0	0	4	0
	BT	0	0	0	0	0	0	0	0	0	0
	MW	0	0	1	0	0	0	0	0	0	0

Of the eight RSPF models that were fit, AIC selected model m6 as the best model with 85% of the AIC weight (Table 5) and contained covariates for mountain whitefish and bull trout presence and an interaction between temperature and habitat type (run, riffle, pool). Model m7, which held 15% of the AIC weight, also included an interaction between bull trout and mountain whitefish presence with habitat area. Therefore, the main uncertainty between the selection of the two models is related to the interaction between bull trout and mountain whitefish presence.

Table 5. AIC table describing model definitions and selection of candidate RSPF models.

Model	Call	df	AIC	dAIC	wAIC	cumAIC
m6	GR01 ~ BT01 + MW + run.area*mtemp + riffle.area*mtemp + pool.area*mtemp	10	96.92	0.00	0.85	0.85
m7	GR01 ~ BT01*pool.area + BT01*run.area + BT01*riffle.area + MW*pool.area + MW*run.area + MW*riffle.area + run.area*mtemp + riffle.area*mtemp + pool.area*mtemp	16	100.36	3.44	0.15	1.00
m5	GR01 ~ BT01 + MW + run.area + riffle.area + pool.area	6	117.95	21.02	0.00	1.00
m3	GR01 ~ BT01 + MW + mtemp + run.area + riffle.area + pool.area	7	119.70	22.78	0.00	1.00
m4	GR01 ~ BT01 + MW + mtemp + sub.fines + sub.cobble + sub.bedrock	7	181.88	84.96	0.00	1.00
m2	GR01 ~ BT01 + MW + mtemp	4	275.17	178.24	0.00	1.00
m0	NULL	0	332.96	236.03	0.00	1.00
m1	GR01 ~ mtemp	2	336.69	239.76	0.00	1.00

RSPF results indicated Arctic grayling selection for pool habitats, negative selection for temperature (indicating selection for cooler water), and selection for co-occurrence with mountain whitefish. Arctic grayling selection for pools of all sizes (small, medium, and large pools representing the 0.1, 0.5, and 0.9 quantiles of the total proportion of reach area, respectively) was low when neither bull trout nor mountain whitefish were present (Figure 20, panel 1). When only mountain whitefish were present, Arctic grayling selection for small, warm pools and large, cool pools was high. Arctic grayling were equally likely to

select medium pools across all temperatures (Figure 20, panel 2). When only bull trout were present in pools, selection was low (Figure 20, panel 3). When both bull trout and mountain whitefish were present, selection for cool pools of all sizes was high, but declined in large pools as they warmed (Figure 20, panel 4).

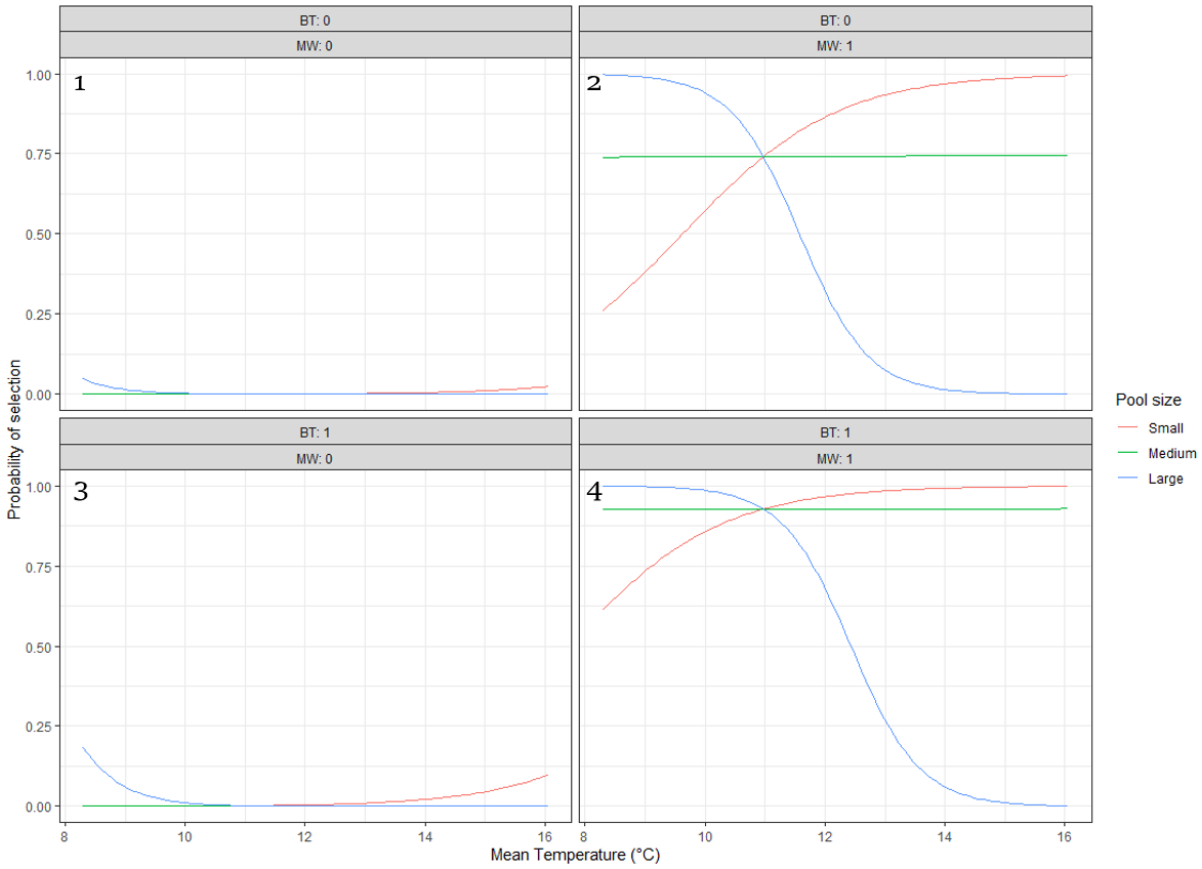

Figure 20. Selection curves of Arctic grayling for pools of three size classes in the presence and absence of bull trout (BT) and mountain whitefish (MW).

The riverscape drone survey produced 52 km of continuous imagery of both the physical habitats and local thermal distributions in the Anzac River (Figure 21).

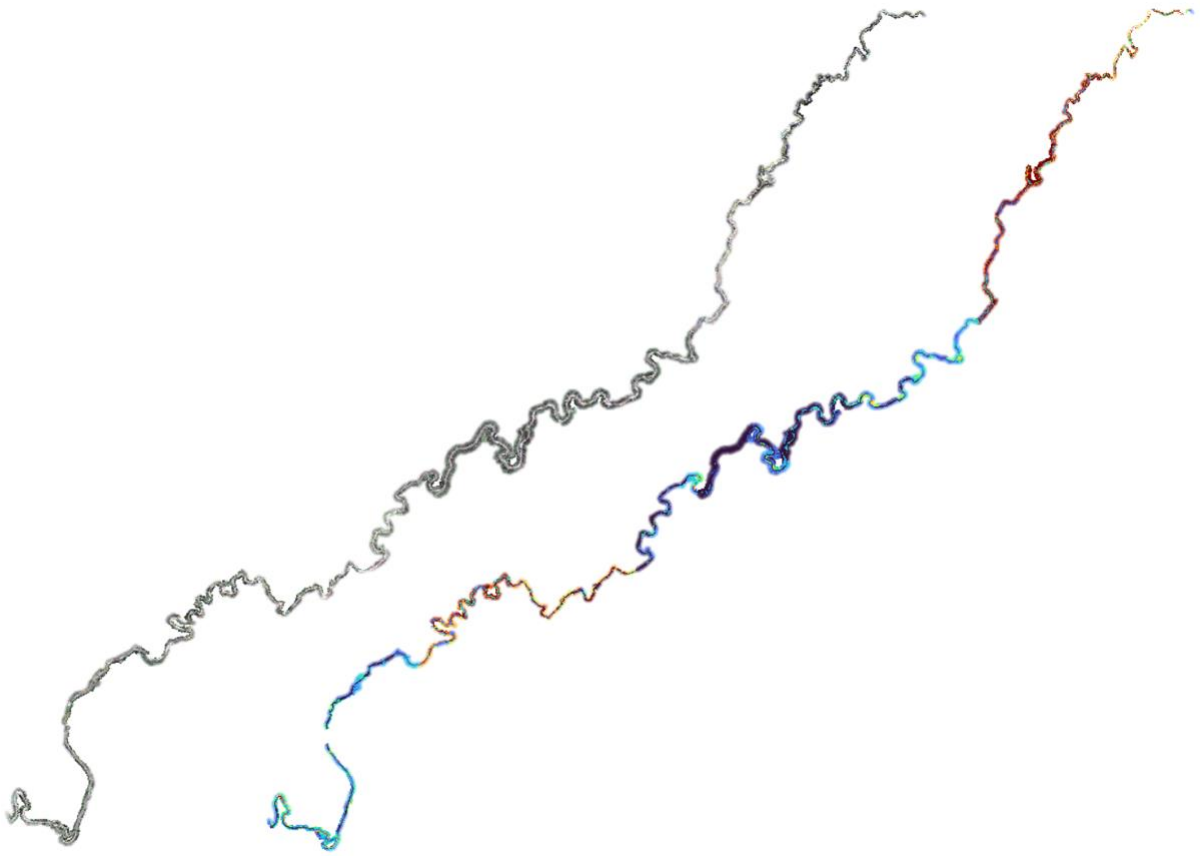

Figure 21. The riverscape survey produced 52 kilometers of physical and thermal images of the Anzac River. Note that due to the mapping occurring over several days, thermal distributions are relevant at local scales only and are subject to local conditions and are not comparable along the latitudinal length of the river.

The pool survey identified 487 pools in the surveyed extent of the Anzac River, with a mean Rkm pool score of 3.26 (Figure 22). The spatial distributions of pool scores across Rkm showed no significant patterns with respect to the latitudinal length of the river, though aggregating across different spatial scales revealed a weak but insignificant trend of increasing scores with upstream distance at the 1 Rkm aggregation scale and decreasing scores with upstream distance when aggregated by 5 and 10 Rkm (Figure 23).

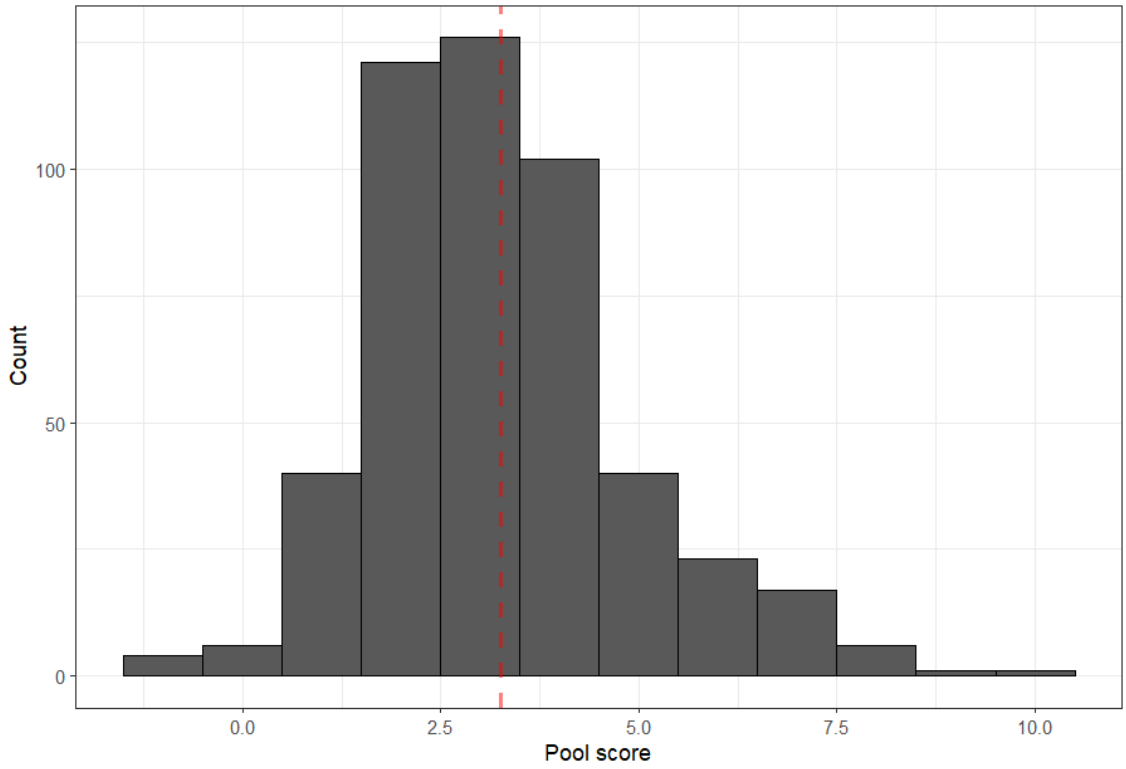

Figure 22. Distribution of pool scores from the riverscape survey.

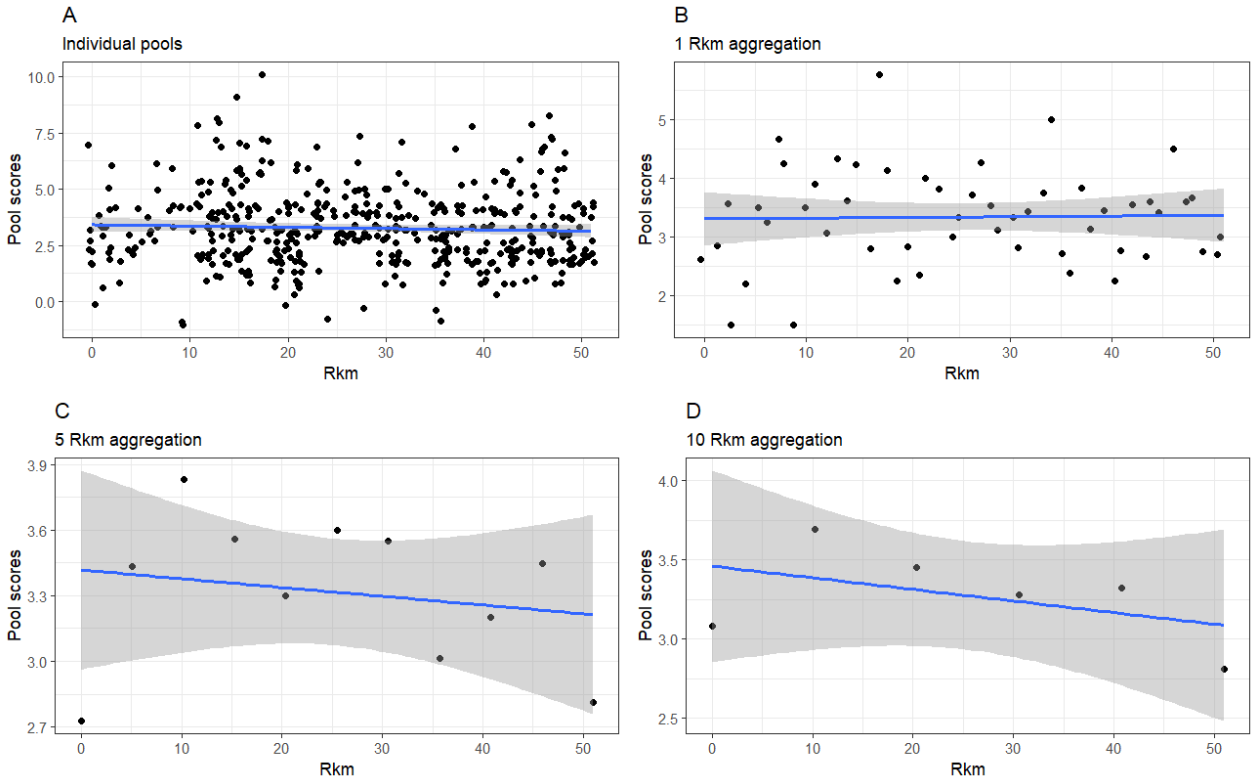

Figure 23. Pool index scores in the Anzac River, aggregated at four spatial scales.

Histograms of pool scores by Rkm (Figure 24) revealed several areas in which clusters of neighboring reaches scored higher than those surrounding them. In particular, reaches between Rkm ranges 7-8, 11-15, 17-18, 22-28, 32-34, 37-39, and 44-48 were identified as high-quality reaches with regard to Arctic grayling habitat potential (Figure 25).

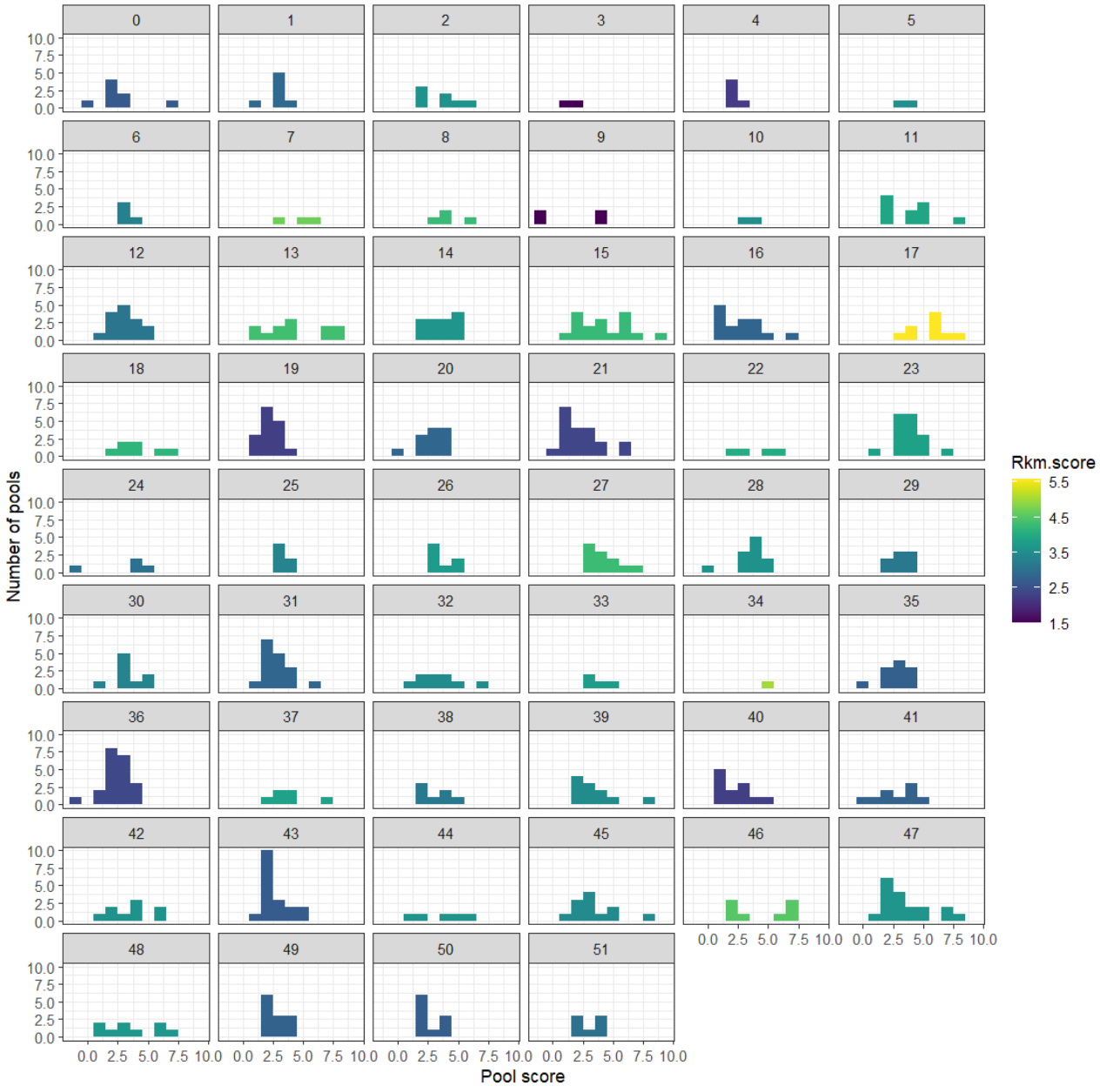

Figure 24. Individual and mean pool index scores aggregated by Rkm. Facet labels correspond to Rkm. Aggregates of consecutively high-scoring reaches can be seen in Rkms 7-8, 11-15, 17-18, 22-28, 32-34, 37-39, and 44-48.

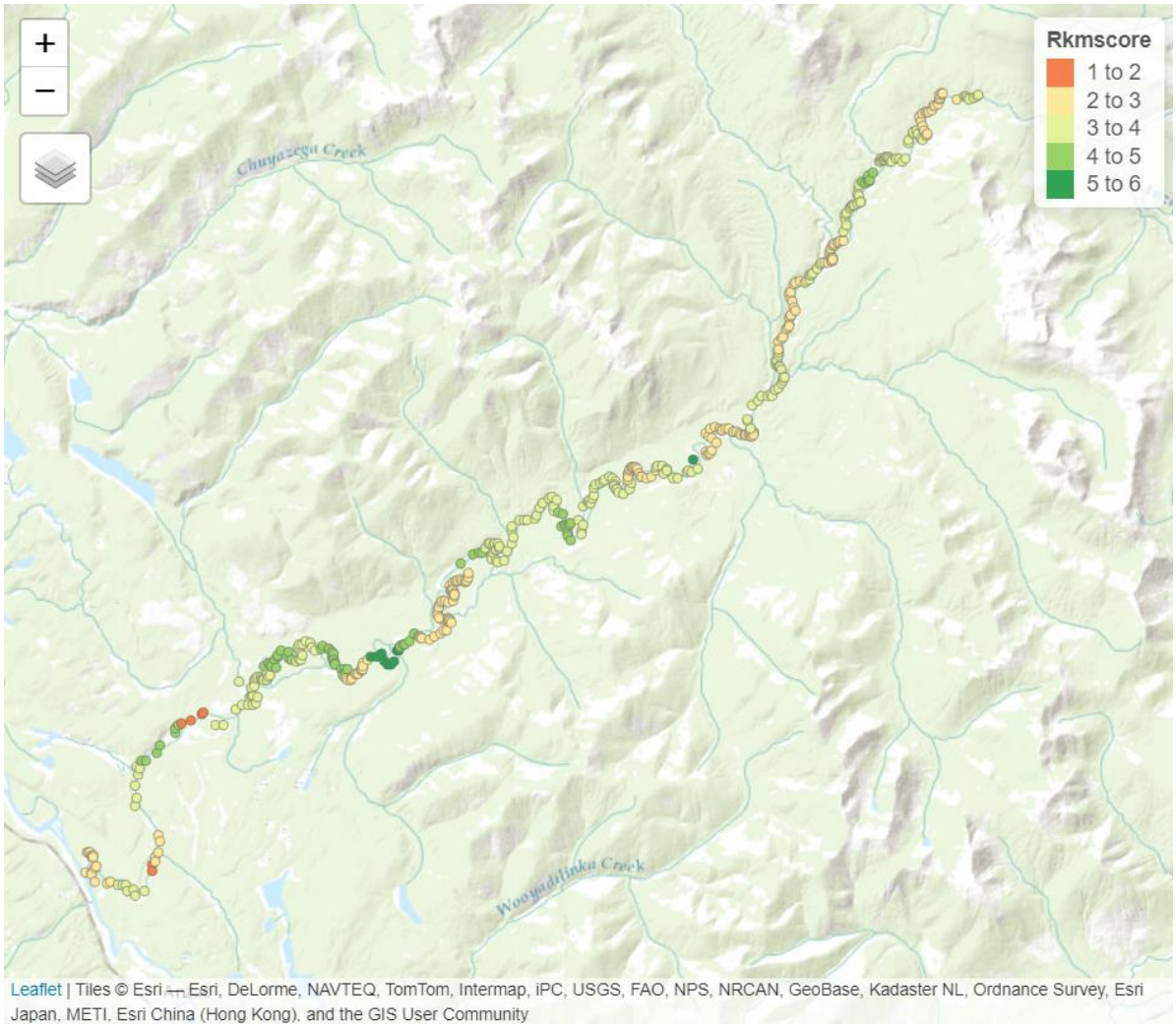

Figure 25. Landscape-level pools, aggregated and color-coded by mean Rkm pool index score.

Arctic grayling population estimates from the John Hagen and Associates snorkel data was regressed against both Rkm-level pool scores and Rkm which revealed a positive but not statistically significant relationship with both covariates (Figure 26). A basic extrapolation of this regression predicted an abundance estimate of Arctic grayling per reach based on reach scores (Figure 27).

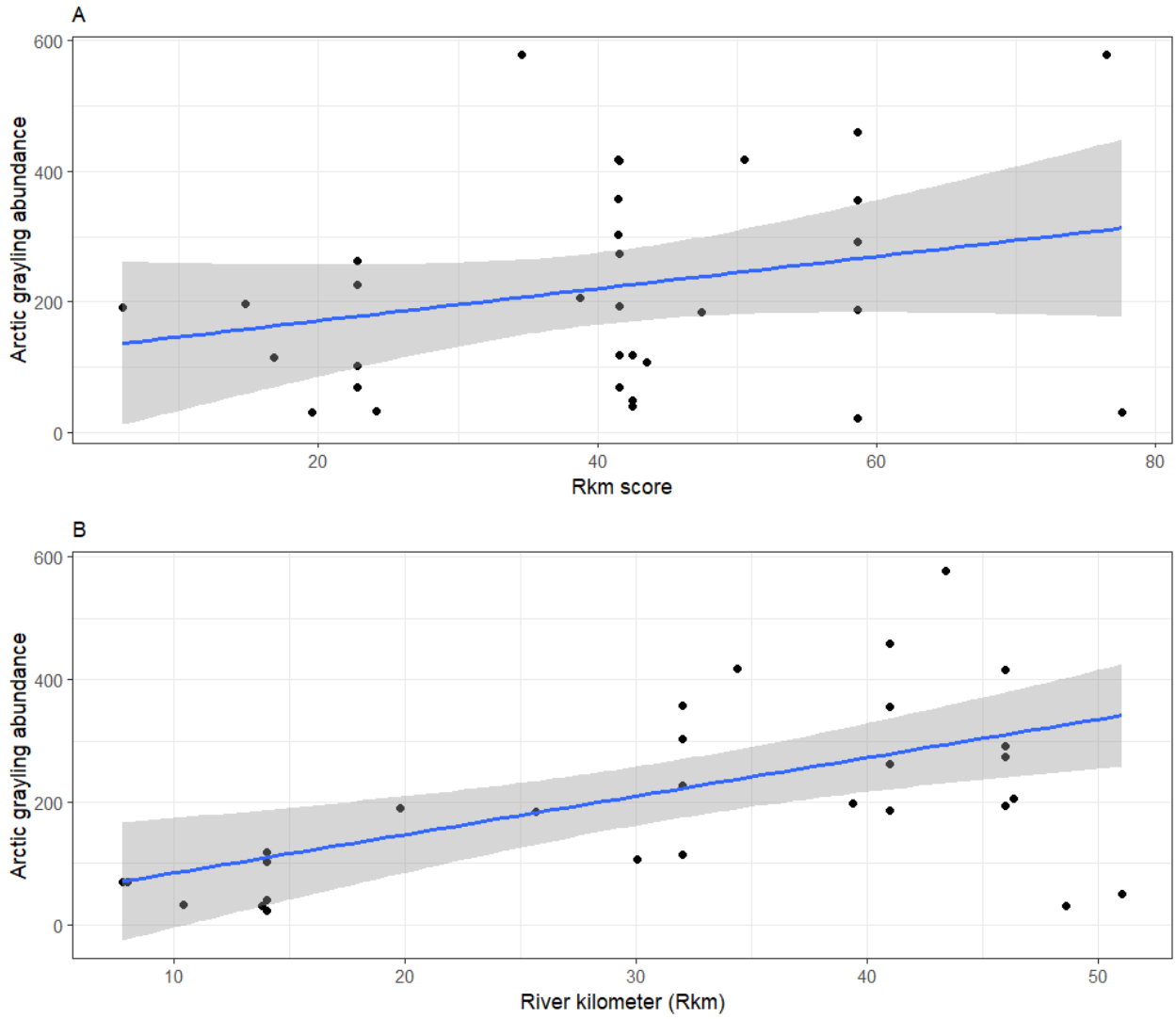

Figure 26. Arctic grayling population estimates from the snorkel surveys conducted by John Hagen and Associates regressed against pool scores at 1 Rkm aggregations (Panel A) and Rkm (Panel B).

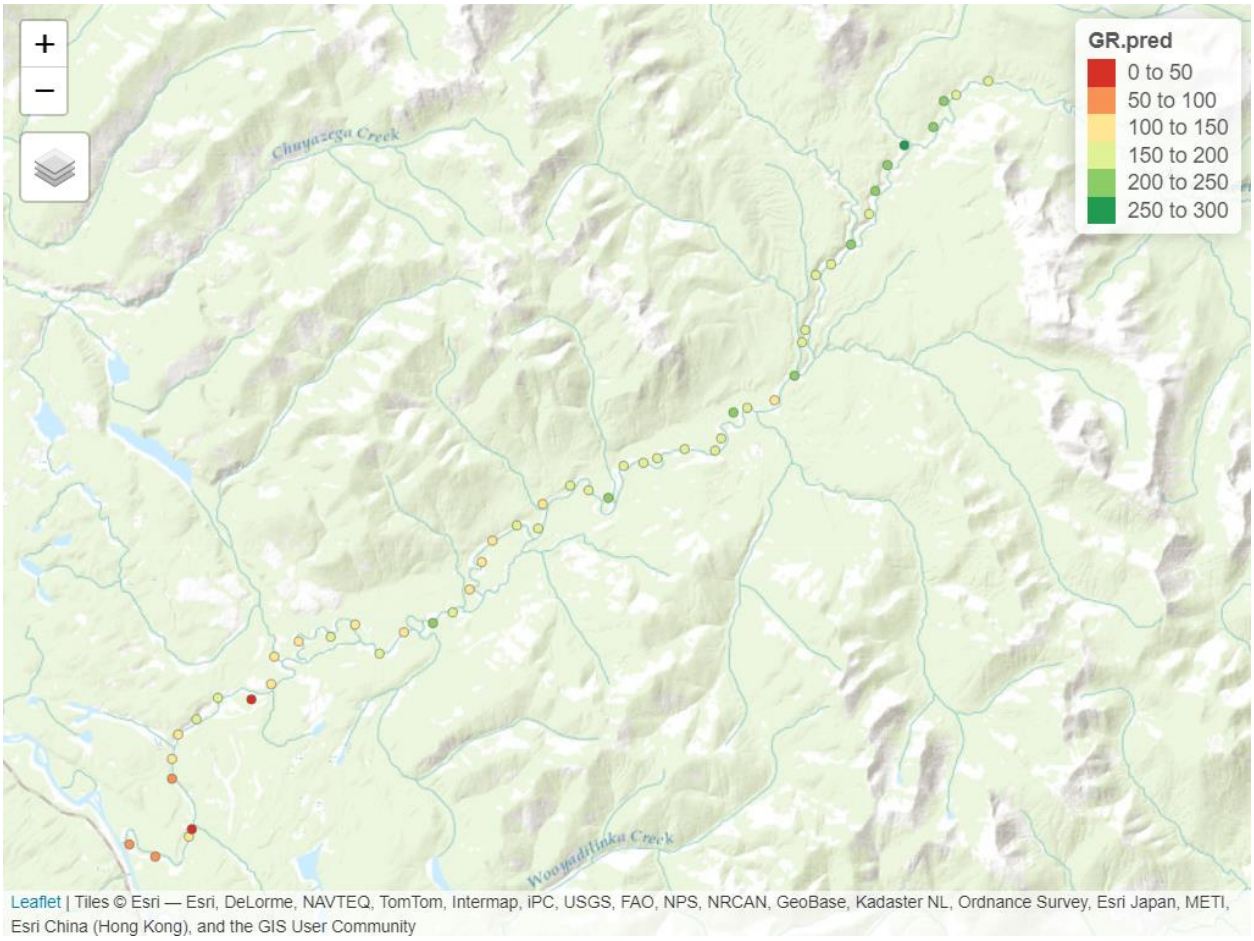

Figure 27. A general extrapolation of the regression model of the Hagen snorkel surveys against pool scores by Rkm. Model included both Rkm score and Rkm as linear predictors of Arctic grayling abundance.

Climate change forecasting

Median river temperatures from the drone images were scaled to various warming scenarios as an exploration into how currently available thermal habitats may contract over time given the cumulative impacts of climate change or future land use changes in this system. Note that warming scenarios are generalized; they do not make use of a specific climate model to account for the different weights of cumulative factors in this system (e.g., canopy loss over low-order tributaries). At a median river temperature of 14 °C, 17% of available thermal habitats in the Anzac River fell within the thermal preference range T_{SET} as determined by the shuttlebox study. Under the 0.5 °C warming scenario, thermal habitat distributions shrank to 9%. Ranges shrank further under the 1.0 °C and 1.5 °C warming scenarios to just 5% and less than 1% of available thermal habitats, respectively (Table 6).

Table 6. Percentages of thermal habitats available within T_{SET} under three future warming scenarios.

Scenario	Percentage of habitat area within T_{SET}
Baseline (14 °C)	16.9
0.5 °C warming	8.6
1.0 °C warming	4.7
1.5 °C warming	0.6

Shuttlebox experiments

The thermal preference and thermal preference range, T_{PREF} and T_{SET}, respectively, were 11.6 °C with a lower bound of 10.1 °C and an upper bound of 13.0 °C (Table 7). T_{PREF} was found to be lower in females (10.5 ± 2.5 °C; n = 6) than males (13.3 ± 3.5 °C; n = 4) and a positive trend was found between T_{PREF} and fork length (Figure 28).

Table 7. Biometrics of the ten fish used in the shuttlebox experiments for thermal preference.

Trial	Date	Capture time	Capture temp (°C)	Fish no.	Sex	Len. (mm)	Wt. (g)	T_{OCC} (°C) q25	T_{OCC} (°C) q50	T_{OCC} (°C) q75
1	2022-08-28	09:35	9.8	53	F	312	360	11.6	12.6	13.2
2	2022-08-29	20:18	12.2	54	F	332	490	10.5	11.3	12.8
3	2022-08-31	08:35	9.1	55	M	353	660	7.0	7.6	8.4
4	2022-09-02	15:15	14.4	56	F	343	500	7.4	9.0	9.7
5	2022-09-03	18:10	13.9	57	F	293	350	6.2	7.2	9.6
6	2022-09-05	07:50	9.1	58	M	362	540	17.6	18.4	18.8
7	2022-09-06	19:07	10.7	59	M	330	425	13.1	14.5	15.5
8	2022-09-08	15:01	10.6	60	F	345	500	9.2	13.9	17.0
9	2022-09-09	16:30	10.2	61	F	304	450	8.0	9.0	9.9
10	2022-09-10	19:36	10.2	62	M	355	500	10.3	12.6	15.2
							$T_{PREF} \pm T_{SET}$:	*10.1*	***11.6***	*13.0*

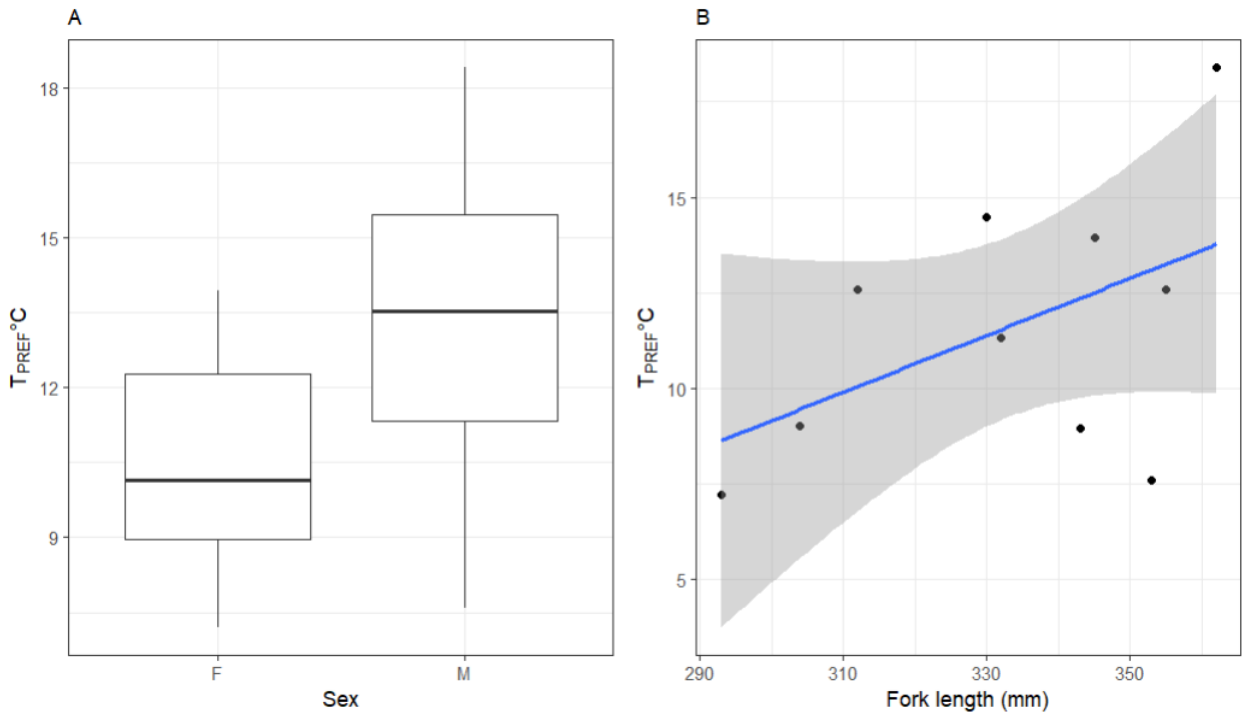

Figure 28. The relationship of T_{PREF} with Arctic grayling sex (panel A) and fork length (panel B).

The model with both centered body weight (*Wc*) and a factor indicating whether the system was warming or cooling (*trend*), was selected as the best model for predicting the heat transfer coefficient *k* (Table 8).

Table 8. AIC table for the nonlinear mixed effects models used to estimate coefficient k.

Model	Fixed effects	df	AIC	BIC	logLik	dAIC	lik	wAIC
mod.all	k ~ Wc + trend	6	-15588.9	-15551.8	7800.4	0.000	1.000	0.875
mod.trend	k ~ trend	5	-15584.0	-15553.0	7797.0	4.926	0.085	0.075
mod.wc	k ~ Wc	5	-15583.0	-15552.1	7796.5	5.890	0.053	0.046
mod.null	k ~ 1	4	-15578.2	-15553.5	7793.1	10.646	0.005	0.004

The intercept of the heat transfer coefficient *k* was estimated as 0.0013 by the top nlme model. Since the top model included centered body weight W_C and the heating or cooling trend variable as fixed effects, predictions of *k* varied based on the weight of the fish and whether their body was heating or cooling. The rate of heat transfer in Arctic grayling decreased with body weight and was overall lower in warming experiments than during cooling experiments (Figure 29).

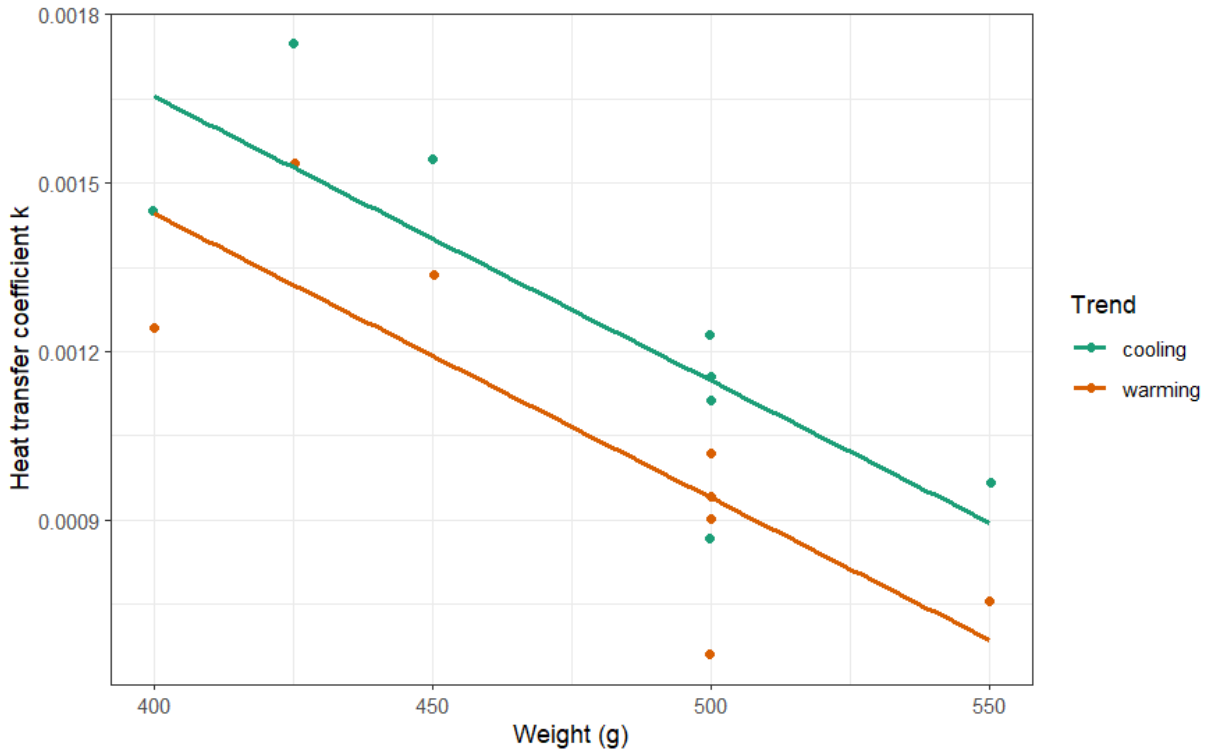

Figure 29. Predictions of the heat transfer coefficient k from the top model which included both centered body weight and a factor indicating whether the experiment was warming or cooling as fixed effects.

Prediction plots were created using coefficient *k* showing the response of Arctic grayling body temperatures over time to both a warming and cooling temperature differential. In both cooling and warming experiments, the rate of heat transfer was greater as the temperature differential increased and decreased as temperatures began to converge. Temperatures converged to ± 0.1 °C under all scenarios around 45 minutes after exposure to the temperature shift (Figure 30).

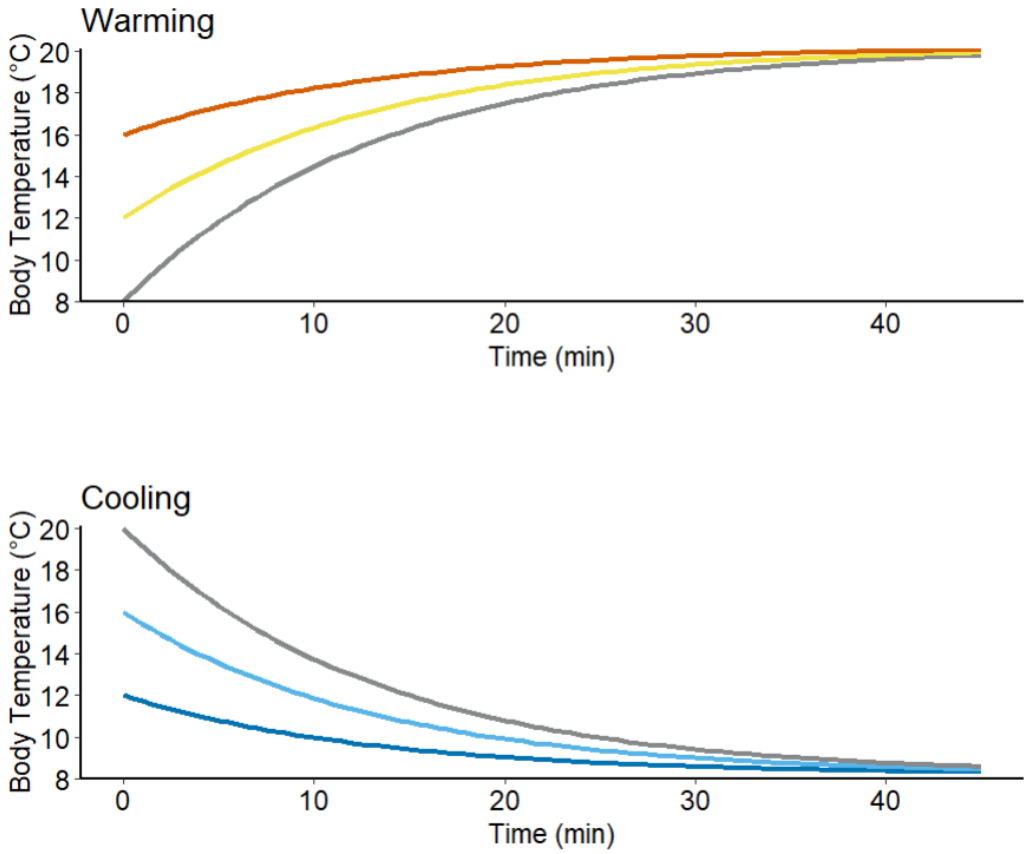

Figure 30. Theoretical response curves based on estimated coefficient k of Arctic grayling to body and ambient temperature differentials under warming and cooling scenarios. The warming plot depicts how Arctic grayling with initial body temperatures of 8, 12, and 16 °C respond to exposure to 18 °C water, and the cooling plot shows how Arctic grayling with initial body temperatures of 20, 16, and 12 °C respond to exposure to 8 °C water.

Biologging with radio telemetry

Of the 50 tags deployed, 42 returned usable data; two were filtered for mortality or early detachment, two were filtered for early emigration from the study reach after tagging, and four were filtered for unclear signal (cases in which a joint inspection of body temperature, ambient temperature, index *E*, and *VeDBA* produce uncertain data, possibly resultant from multiple filtering, see Discussion and Appendix 1). The tags that produced usable data had an average continuous time series length of 311 hours (minimum 6, maximum 985; Figure 31) A summary of tag deployments can be found in Table 9.

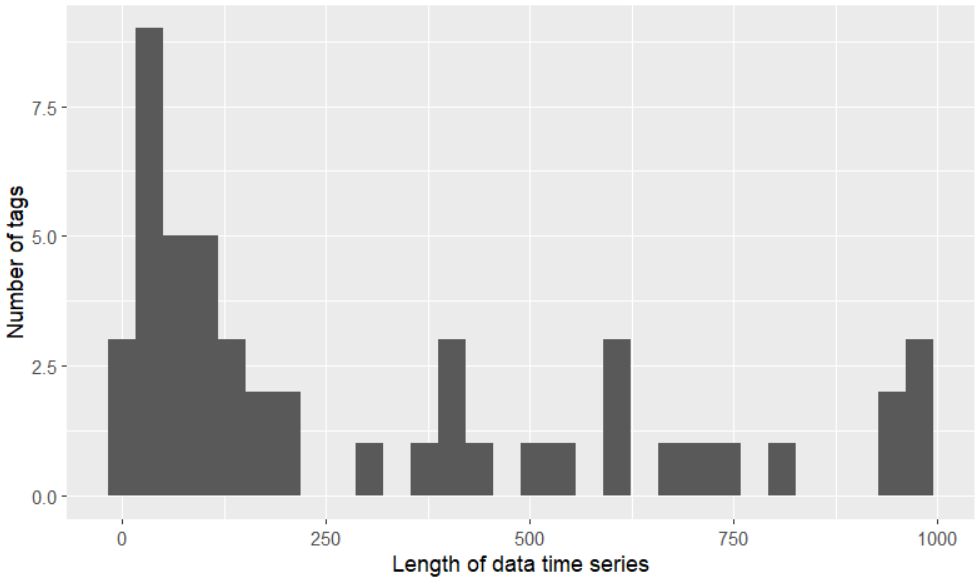

Figure 31. Histogram of length in hours of continuous time series data produced by the radio tags in this study.

Table 9. Summary table of the 50 Arctic grayling which received radio tags.

Date	Time	Reach	Fish no.	Sex	Len. (mm)	Wt. (g)	Floy no.	Radio no.
2022-07-28	13:56	A	1	F	330	415	438	19
2022-07-28	14:09	A	2	M	361	420	439	22
2022-07-28	14:20	A	3	M	365	430	440	21
2022-07-28	14:30	A	4	F	359	430	441	24
2022-07-28	14:42	A	5	F	345	420	442	20
2022-07-28	14:45	A	6	F	314	320	443	27
2022-07-28	15:09	A	7	M	340	490	444	25
2022-08-05	13:37	B	8	M	380	650	445	8
2022-08-05	13:46	B	9	-	318	350	446	17
2022-08-05	14:09	B	10	-	395	700	338	15
2022-08-05	14:30	B	11	-	321	300	449	7
2022-08-05	14:46	B	12	-	340	490	450	16
2022-08-05	15:02	B	13	-	345	450	520	26
2022-08-05	15:16	B	14	-	346	450	527	28
2022-08-05	15:45	B	15	M	350	450	530	1
2022-08-05	18:19	B	16	F	352	575	528	4
2022-08-05	18:37	B	17	F	310	375	531	2
2022-08-05	18:47	B	18	M	324	400	532	6
2022-08-05	18:56	B	19	M	316	400	533	18
2022-08-06	13:44	A	20	F	309	340	534	13
2022-08-06	18:28	A	21	-	323	675	535	5
2022-08-06	19:11	B	22	M	408	800	537	12
2022-08-06	20:52	B	23	F	310	610	538	14
2022-08-06	21:04	B	24	-	354	780	539	11
2022-08-07	12:27	B	25	M	337	640	540	10
2022-08-07	12:33	B	26	M	338	799	541	3
2022-08-07	12:39	B	27	F	310	620	542	9
2022-08-07	12:45	B	28	M	313	640	543	23
2022-08-13	17:13	B	29	M	340	390	544	31
2022-08-13	17:18	B	30	-	350	560	545	32
2022-08-13	17:22	B	31	M	383	580	546	35
2022-08-13	17:35	B	32	M	375	640	547	29
2022-08-13	17:42	B	33	F	350	500	548	50
2022-08-13	17:53	B	34	F	324	440	549	30
2022-08-13	20:07	B	35	M	328	400	550	33
2022-08-13	20:19	B	36	F	390	440	501	34
2022-08-13	15:33	B	37	-	380	380	502	36
2022-08-13	15:54	B	38	-	307	340	503	37
2022-08-14	20:20	B	39	F	344	510	504	38
2022-08-14	20:25	B	40	M	305	390	505	39
2022-08-14	20:33	B	41	M	325	420	506	40
2022-08-14	20:40	B	42	F	335	460	507	41
2022-08-21	13:52	B	43	F	308	350	508	48
2022-08-21	14:01	B	44	M	398	625	509	42
2022-08-21	14:14	B	45	M	329	400	510	43
2022-08-21	14:21	B	46	F	299	350	511	46
2022-08-21	14:30	B	47	M	370	550	514	44
2022-08-21	15:18	B	48	M	389	600	515	45
2022-08-21	15:27	B	49	F	328	420	516	49
2022-08-21	15:37	B	50	F	335	600	517	47

An example of body temperature (predicted based on water temperature data transmitted by the tags and the heat transfer equation developed in this study), VeDBA and index *E* (computed based on body temperature and water temperature availability data) is shown in Figure 30. This figure depicts summary data for radio tag number 25, a 340 mm male Arctic grayling radio tagged in reach A on July 28, 2022. The three plots represent body temperatures against the range of ambient temperatures and the T_{SET} range determined by the shuttlebox study (top), the diel pattern of index *E* over time (middle), and the maximum hourly values of *VeDBA* (lower). Visible in this example plot is the lag between the tagging date on July 28 and the first detections around study hour 100 (when the receiver in this particular reach came online after a manufacturer programming error was corrected); a switch between efficient and inefficient behavioral thermoregulation around study hour 300, when ambient temperatures began non-overlapping diel patterns with respect to the T_{SET} range, and more frequent nighttime thermoregulatory behavior after hour 850; and generally low values of *VeDBA* throughout the period punctuated with bursts of higher activity which don't have a clear visual pattern with plots of index E or body temperature. Similar plots for all fish with usable data can be found in Appendix 1.

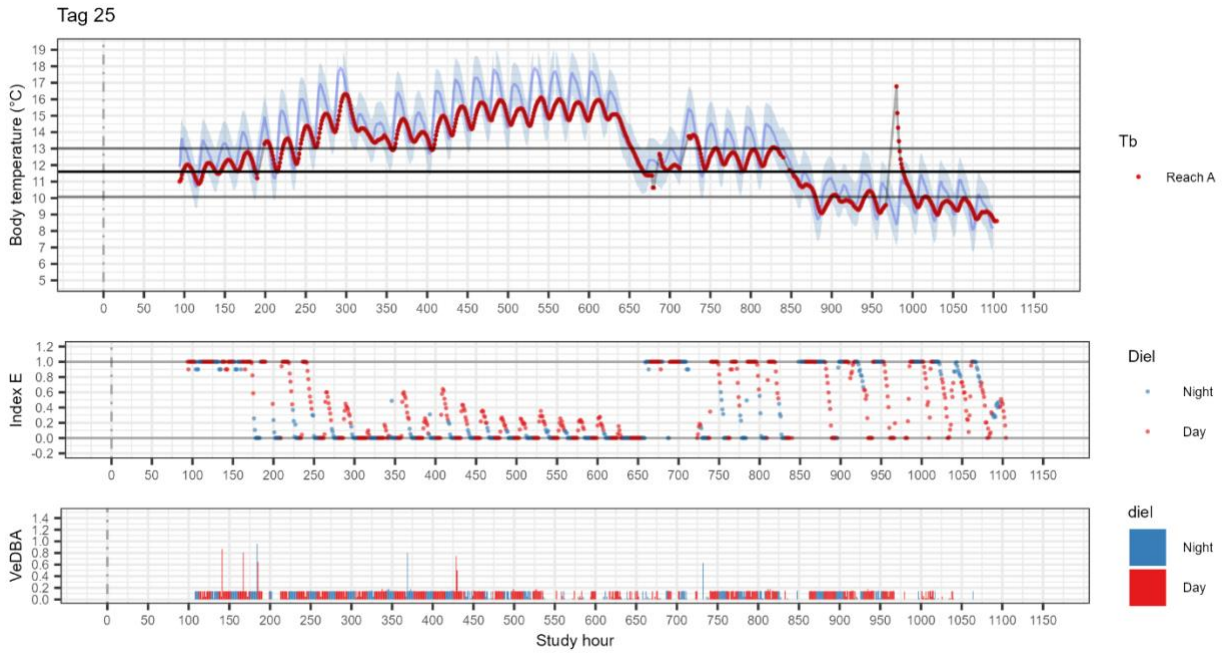

Figure 32. Example radio tag inspection summary. Vertical dashed line is the radio tagging date. The blue line and shaded region represent median ambient water temperatures ± 1 SD. Black horizontal lines in the body temperature plot denote the thermal preference range T_{SET} as determined by the shuttlebox study. Note the suspected angler recapture event around study hour 1,000 where temperatures drastically deviate from ambient ranges and quickly return after the event.

Index *E* varied through time with tagged Arctic grayling actively thermoregulating during the day during the hot early season and thermoconforming at night. This pattern switched as ambient temperatures dropped below the T_{SET} range in early September, with individuals actively thermoregulating at night and thermoconforming during the day (Figure 33). When ambient temperatures within the T_{SET} range did not exist at any time of day or night, Arctic grayling attempted to thermoregulate during the day (inefficiently) and thermoconformed at night (Figure 33). Models of index *E* indicated that relative bull trout abundance did not affect index *E*. Over the duration of the study, metric E_X indicated that sampled Arctic grayling exploited their T_{SET} range 81% of the time that it was available.

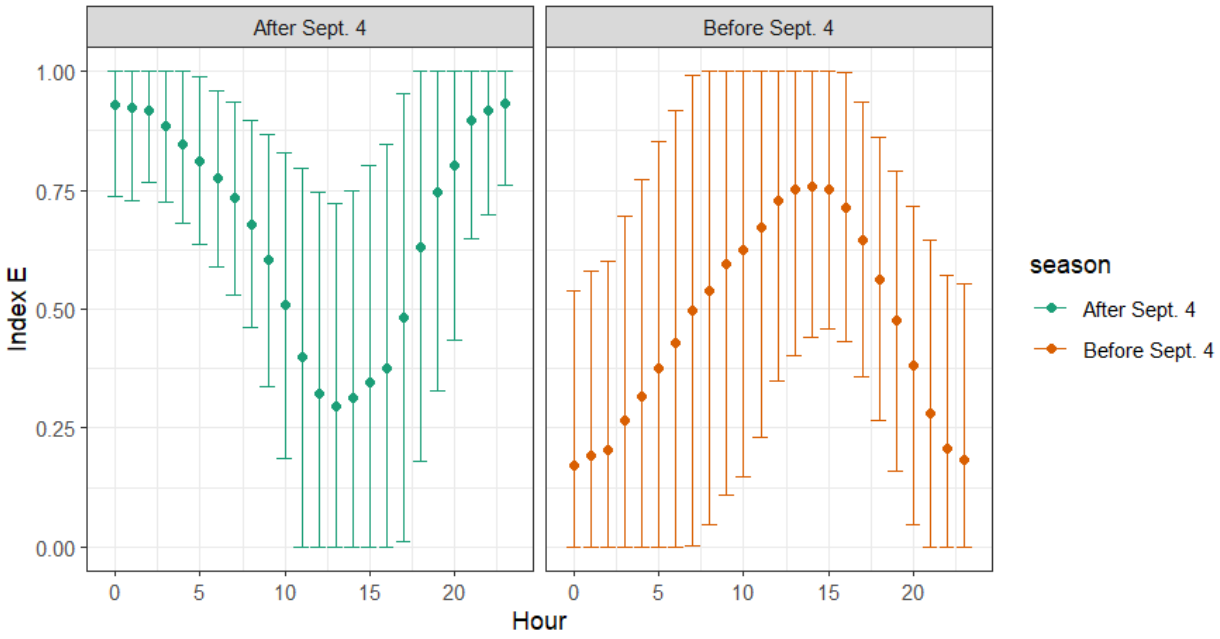

Figure 33. Mean hourly Index E patterns before and after September 4. Error bars represent the hourly mean +- 1 SD and are capped where they overlap with the index E limits of 0 and 1.

The top two index *E* models selected by AIC together held a cumulative weight of 1 and were averaged to produce a single predictive model containing covariates for mean ambient water temperatures, VeDBA, hour of day, habitat patchiness, and body condition (Table 10).

Table 10. AIC selection table of candidate GAMMs fit in this analysis.

Model	Call	df	AIC	dAIC	lik	wAIC	cum_wAIC
gam17	logit(E) ~ VeDBA + Patchiness + Hour + mTemp	10	27940	0.00	1.00	0.865	0.865
gam25	logit(E) ~ VeDBA + Patchiness + Hour + mTemp + K	12	27939.43	3.72	0.16	0.135	1.000
gam18	logit(E) ~ VeDBA + Hour + mTemp	8	27965	24.71	4.33E-06	3.7E-06	1.0
gam9	logit(E) ~ mTemp + Hour	6	27969	28.96	0.0	0.0	1.0
gam8	logit(E) ~ BT	6	29629	1688.88	0.0	0.0	1.0
gam7	logit(E) ~ mTemp + Patchiness	7	29703	1762.66	0.0	0.0	1.0
gam19	logit(E) ~ VeDBA + Patchiness + mTemp	9	29706	1765.95	0.0	0.0	1.0
gam6	logit(E) ~ mTemp	5	29746	1805.14	0.0	0.0	1.0
gam2	logit(E) ~ VeDBA + mTemp	7	29749	1808.52	0.0	0.0	1.0
gam14	logit(E) ~ BT + Hour	5	29880	1939.96	0.0	0.0	1.0
gam12	logit(E) ~ Patchiness + Hour	6	29904	1963.36	0.0	0.0	1.0
gam16	logit(E) ~ VeDBA + Patchiness + Hour	8	29906	1965.19	0.0	0.0	1.0
gam15	logit(E) ~ Hour	4	30359	2418.06	0.0	0.0	1.0
gam5	logit(E) ~ VeDBA + Hour	6	30361	2420.74	0.0	0.0	1.0
gam11	logit(E) ~ Patchiness + BT	6	30806	2865.59	0.0	0.0	1.0
gam20	logit(E) ~ VeDBA + Patchiness + BT	8	30808	2867.98	0.0	0.0	1.0
gam13	logit(E) ~ BT	4	31099	3158.95	0.0	0.0	1.0
gam4	logit(E) ~ VeDBA + BT	6	31102	3161.93	0.0	0.0	1.0
gam10	logit(E) ~ Patchiness	5	31163	3222.21	0.0	0.0	1.0
gam3	logit(E) ~ VeDBA + Patchiness	7	31166	3225.25	0.0	0.0	1.0
gam24	logit(E) ~ Patchiness + K	7	31166	3225.64	0.0	0.0	1.0
gam21	logit(E) ~ VeDBA + Patchiness + K	9	31169	3228.66	0.0	0.0	1.0
gam0	logit(E) ~ 1 (NULL)	3	31552	3611.24	0.0	0.0	1.0
gam22	logit(E) ~ VeDBA + K	5	31555	3614.51	0.0	0.0	1.0
gam23	logit(E) ~ K	5	31555	3614.51	0.0	0.0	1.0
gam1	logit(E) ~ VeDBA	5	31555	3614.75	0.0	0.0	1.0

The covariates in the averaged model with the largest effect size on thermoregulatory efficiency were temperature and hour of the day (Figure 34) which showed an inverse relationship to one another. The positive effect of mean ambient water temperatures on thermoregulatory efficiency is most pronounced when temperatures just exceeded the upper bound of the T_{SET} range (around 14 °C) and were lower when ambient temperatures were at, below, or far exceeding T_{SET} (Figure 32A). Similarly, the negative effect of hour of the day on thermoregulatory efficiency was most pronounced around 16:00, when daily water temperatures were at their maximum (Figure 32C). Thermoregulatory efficiency increased with VeDBA and was most efficient around 0.75 (Figure 32B), with efficiency decreasing as VeDBA increased and showing a small positive trend at the highest levels of activity (Panel B). Habitat patchiness had the greatest effect size on thermoregulatory efficiency when patchiness tended towards extremes, with a smaller effect on moderately patchy habitats, though the overall effect size was small (Figure 32D). Thermoregulatory efficiency had a weakly positive relationship with body condition, indicating that fish with a higher body condition were more efficient thermoregulators (Figure 32E).

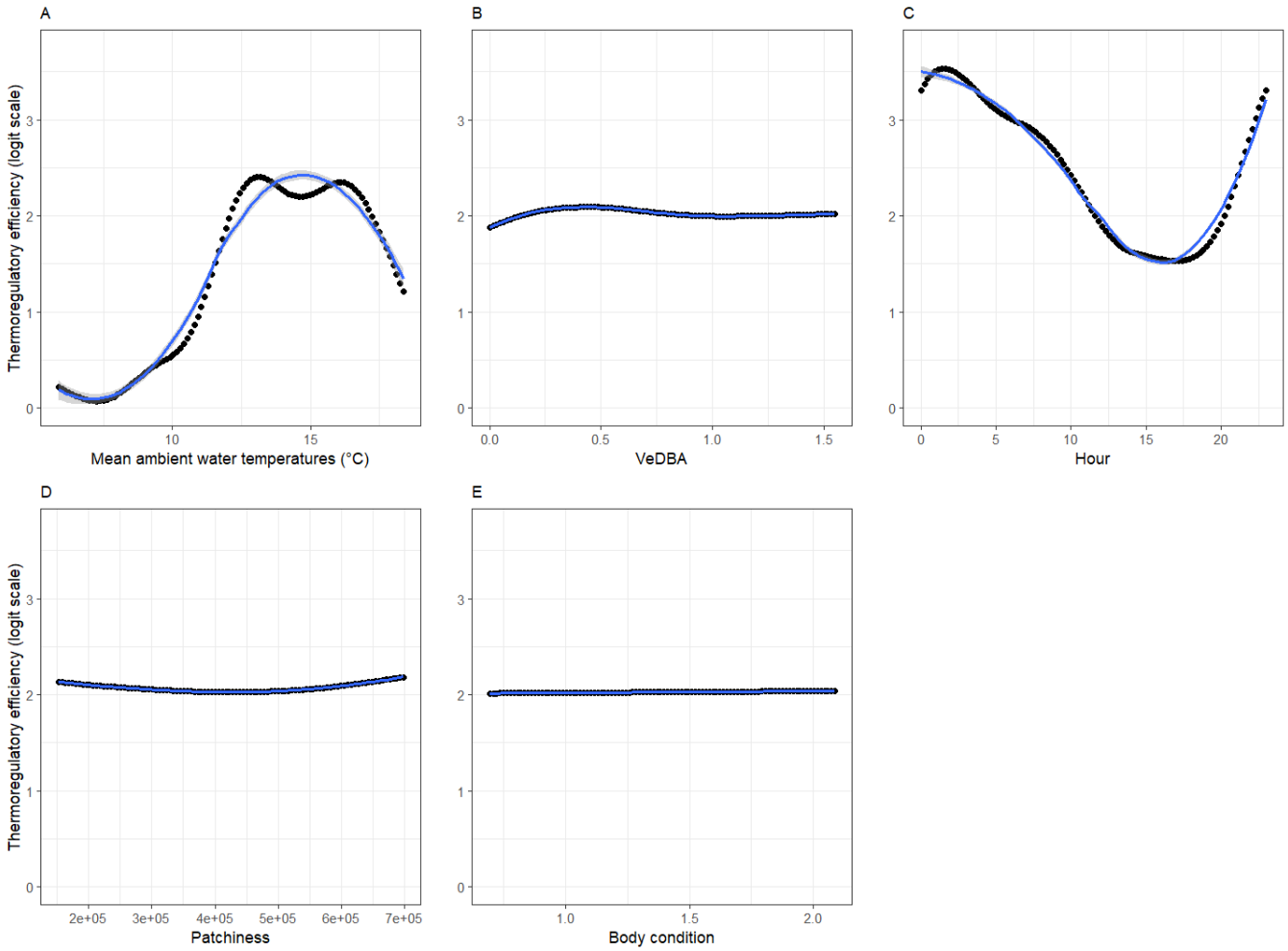

Figure 34. Model averaged outputs from the relationships identified in the selected GAMM models. Index E in these models used a logit transformation.

6. Discussion

This study examined the thermal ecology of adult Arctic grayling during the summer feeding season in the Anzac River. In pursuit of a well-rounded picture of a complex system, we examined the intersection between thermal habitat use/selection, preference, and availability. Each method and study design used in these investigations came with its own set of parameters and constraints in both spatiotemporal grain and extent. In riverine ecology, it is important to contextualize studies at reach scales to the greater riverscape as river habitats are connected through a continuum of patterns and processes from headwaters to mouth and few observable relationships are truly independent of upstream or downstream factors (Vannote et al. 1980). The examination of behaviors in this study was conducted during a time when Arctic grayling display territorial holding patterns (McPhail 2007, Hughes 1998), the spatial extent of which is relatively small and amenable for this *in situ* study. By having our study window and available tools overlap with John

Hagen and Associates' long-term index reach snorkel study, we had the opportunity to extend the findings from our reach-scale study to the greater riverscape.

The Anzac River is a shifting gravel-bed ecosystem which is in places subject to dramatic changes during annual hydrologic cycles and discrete events such as storms and freshet. In the five field seasons this team has spent studying this system, the 2022 field season presented some of the most favorable conditions for aerial imaging and snorkel surveys; it was as close to a 'typical' year one could hope for. Freshet was tailing off right as the study began in late July. Rainfall events happened, preventing the severe drought conditions and thermal stressors of some years (2018, 2021), but not at the frequency or severity as in some other years (2019, 2020). While this was good for being able to collect drone imagery and conduct work in the river, it had some implications for the types of data that were collected at different resolutions. Relatively low water constricted surveyable habitats in the study reaches to deeper runs and pools. While it is highly likely that some habitat use occurred in micro-pools along cobbly riffles, it went largely unobserved during our snorkel surveys in which some shallow reaches were walked more than they were swam. The same can be said of subreach habitats along the bedrock chute in reach B which, as a constricted canyon, was sensitive to small changes in flow and was only surveyed fully under the lowest conditions. While habitat constrictions associated with the relatively low water were not experienced equally throughout the riverscape, the relationships between Arctic grayling and their habitats were defined at the reach-scale and inferences about their habitat availability across the greater riverscape should be understood in that context.

Drone and snorkel surveys

For the RSPF models, we followed a used-available design in which known occupied habitats were compared against all available habitats. This approach allowed for it to be unknown whether an area of available habitat is used or not but lacked true zero observations across all available habitat-covariate combinations (Lele and Keim, 2006). This is contrasted against the used-unused design in which confirmation of unused habitats is required (Johnson *et al.*, 2006). To illustrate the above point regarding applying reach-scale inferences to the greater riverscape, consider the relationship between Arctic grayling and mountain whitefish, which was found to be strongly positively associated by the RSPF analysis. This could be inferred to mean that they share habitat selection criteria, or that they select to co-occur with each other through some trophic relationship. Considering that whitefish were included in this study as a potential competitor, a positive association could indicate that co-occurrence with mountain whitefish may not be competitively detrimental to Arctic grayling and that adaptive behaviors of both species can permit habitat sharing (Nakano 1998).In the case of this study, it is likely that this association may result from a combination of overlapping habitat needs and low flows concentrating species into pool and run habitats. Though the relationship with mountain whitefish was ultimately inconclusive, the positive association between Arctic grayling and pool habitats, particularly large cool ones, is perhaps unsurprising. It is well understood that fluvial Arctic grayling feed off terrestrial drift (McPhail 2004), which is abundant in pool habitats beneath riffles which sweep terrestrial insects into the flow. While mountain whitefish are not a good predictor

of Arctic grayling habitat use across the riverscape, the association between Arctic grayling and pool habitats can be considered relevant to larger scales and is supported by past work (strong associations were found with pools in >60% of cases; Stamford et al. 2017, Blackman 2002, Zemlak and Langston, 1998).

Associations between Arctic grayling and run habitats were present but weak in some of the models we fit and may have been evidence of a weak signal from this dataset that could emerge with a larger sample size. This could be related to the relatively low flows in 2022 restricting most of the usable habitats to pools. It could have also been a function of how habitat layers were defined. Automated GIS workflows for riverine habitat delineation are limited with respect to the combination of sensors we had on board the drone, and as such habitat areas used in the RSPFs were defined manually for each study reach and subjective determinations based on drone orthomosaics and site knowledge and decisions about where run habitat ended and pool habitat began could have influenced model predictions.

The investigations into the trophic relationship between Arctic grayling and bull trout in this system have been ongoing since well before this study (Stamford et al. 2017; Martins et al. PEA-F21-F-3178). The prior study by Martins et al. found through stable isotope analysis that bull trout are consuming prey at the same trophic level as Arctic grayling but was inconclusive on a definitive predator-prey relationship between the species. Spatial capture-recapture modeling done as part of the same study found associations between watershed-scale bull trout and Arctic grayling relative distributions, with similar confounding factors making conclusions about a relationship unclear (Bottoms et al. *Unpublished data*). In this dataset, the low probability of selection in pools with only bull trout in them is in part explained by a lack of surveyed medium and large pools containing only bull trout. If Arctic grayling are indeed significantly depredated by bull trout, it seems sensible that they would not select to share a small pool with a predator. However, positive associations with bull trout were found in some of the unselected RSPFs and a weak association in the selected model could again be a function of low water in 2022 concentrating observable fish in pool habitats. These signals could be further influenced by the schooling effect in which individual predation risk in Arctic grayling is lower when occupying habitats with numerous conspecifics. Further, indices E and E_X showed no change throughout the study area associated with relative bull trout abundance BT_S. While these findings continue to lack strong evidence for a relationship between the species, it could be reasoned from cumulative findings and anecdotal evidence (one bull trout *may* have been observed with a radio tag antenna coming out of its mouth) that the relationship may be opportunistically predator-prey, and Arctic grayling avoid bull trout only when more favorable habitats are available.

The workflows used in this study to produce and analyze drone imagery were produced by manual mapping in lieu of pre-programmed flights due to its relative efficiency compared with slower pre-programmed flights when working at the spatial scales we investigate in this work. This approach comes with tradeoffs, as image orthorectification can be sensitive to variable flight heights, speeds, and image overlap (Wich and Pin Koh 2018). Through use of Pix4DMapper's photogrammetry tools which accommodate variable image overlap, we

were successful in producing high-quality orthomosaics at both the reach and riverscape scales. However, spatiotemporal variation in mapping conditions cannot be controlled entirely. Flights were flown as close as practicable to solar noon, though some images gathered were still subjected to variable shadows due to reach topography or from individual or patchy and diffuse high clouds. We attempted to account for this variation by including the shade parameter when calculating pool scores, though the extent to which thermal signature muting occurred was likely variable based on local conditions and unique pool characteristics. As FLIR sensors such as the one used in this study only measure the surface temperatures of an object, it is possible that deeper pools had more internal thermal heterogeneity than what was represented by surface signatures. We accommodate for this with the depth parameter when calculating pool scores, though data on the degree to which depth and thermal heterogeneity are related in this system were not available. The goal of capturing thermal signatures at solar noon was to produce imagery at the time of day when thermal variation is most exaggerated as light penetrates the entire water column (Casas-Mulet et al. 2020; Dugdale et al. 2015). Analyses which make use of hourly interpolated rasters (e.g. GAMMs in the radio tagging portion of the study) represent hourly temperature measurements from the HOBO logger array as mapped to these high-visibility thermal distributions. These analyses assume that the relative thermal heterogeneities of these reaches persist to some degree beneath the surface throughout the day, though it is possible that the relief of heterogeneous temperatures became muted during overnight lows which would not be represented in the data without the inclusion of night flights to calibrate thermal distributions at a diel resolution. Riverscape-scale mapping captured a snapshot of a large area over a relatively discrete timeframe (4 days, 3 of which were surveyed). Calibration of relative temperature distributions to absolute temperatures (as was done in the reach-scale study) would have required an extensive HOBO logger array which spanned the surveyed extent. Thermal rasters at the riverscape scale as such are relevant to local scales, i.e., examining the internal thermal heterogeneity of discrete habitat features and their adjacent habitats identified in the RGB layer.

Pool ranks were used as an index to apply the findings from our reach-scale RSPF studies to the greater riverscape, though the calculation of this metric does not accommodate other factors known to drive Arctic grayling abundance (e.g., terrestrial drift, Hughes 1998). As such, this approach of indexing pools may artificially bias the importance of pools which have high thermal heterogeneity and/or large size but have relatively homogenous surrounding habitats which do not produce large amounts of terrestrial drift (e.g., large corner pools of relatively slack water). Sampling the riverscape for invertebrate drift as a proxy for spatial forage quality was investigated, though discussion with invertebrate sampling experts concluded that analyses of these data would be massively time prohibitive compared to the amount of information it would add to the analyses at relevant spatiotemporal scales (D. Erasmus, UNBC and C. Cena, EDI, *Personal Communications*). To this end, it is important to note that the pool scoring index developed in this work is extending the results of an RSPF conducted during the summer trophic window when the critical habitat requirements of Arctic grayling are related to feeding (McPhail 2004, Stamford et al. 2017). The inferences made about critical habitats across the riverscape as

such also relate to this timeframe. This index does not score for other Arctic grayling life history stages, which may be equally important through a conservation lens depending on where lifestage bottlenecks occur. For example, pools with thermal signatures warmer than surrounding river temperatures were scored negatively, though this is not indicative of how these pools would be scored for juvenile Arctic grayling seeking to maximize their metabolic rate during critical early rearing (Hawkshaw et al. 2011). Alternately, pool scores in the lowest reaches of the Anzac were low, but these areas are likely critical overwintering habitats in addition to the mainstem Parsnip River (as supported by findings in Martins et al. 2021 (PEA-F21-F-3178); Blackman 2002).

Extending the findings from the John Hagen and Associates snorkel study to the riverscape study in this report was an exploratory venture which yielded interesting results. While the trend between the Hagen team snorkel counts and our pool index aggregated to the 1 Rkm scale showed a clear positive pattern with low residuals (Figure 26), there were only four data points from the snorkel survey available for use in regression. It is possible that with more data a significant result could emerge, though we recognize that this would be onerous and expensive to collect over relevant scales to diminishing returns on new inferences about this population. While we extended these findings to a general predictive model of Arctic grayling abundance per reach (Figure 27), this was ultimately a different way to visualize the pool index through space. It is however interesting to note that 12 of the 14 Rkm index reaches included in the Hagen team snorkel study were also flagged as areas of high conservation potential in the riverscape pool analysis in this study.

Shuttlebox experiments

Considering that Arctic grayling are the coldwater cousins of other more temperate salmonids with well defined T_{PREF} and T_{SET} ranges in the mid-to-high teens, the determined T_{PREF} and T_{SET} range of Arctic grayling in this study of 11.6 °C (10.1 °C - 13.0 °C) presents a reasonable range for montane fluvial fishes in an Arctic watershed. Shuttlebox studies assume that movements between available environments are made behaviorally by choice and not because of external unobserved factors (Christensen et al 2021; Angilletta 2009). Shuttlebox data filters were defined based on a four-hour acclimation period in which the Arctic grayling learned its environment. Experiments in which the Arctic grayling didn't show evidence of interacting with their thermal environment by remaining mostly stationary after four hours were discarded. For example, some individuals would conduct an initial exploratory period and then settle in one tank for the remaining twenty hours, artificially driving thermal preference selection in one direction or the other. Indeed, the failure to filter out these inconclusive experiments is believed to bias shuttlebox studies (Christensen et al. 2021). The ten fish which were successfully trialed for thermal preference showed T_{PREF} ranging from 7.2 C - 18.4 °C, which demonstrates that T_{PREF} is a variable metric within populations subject to the same availability of thermal habitats. It is known that T_{PREF} can vary through time as seasonal habitats fluctuate and fish acclimate to changing thermal conditions and life history strategies require different operational ranges (for example, juvenile grayling were showed to have a T_{PREF} of 16.8 °C (± 0.66 °C), which is optimal for metabolic efficiency during rapid early-life growth; Hawkshaw et al. 2011).

It is however not known at what rate and variability T_{PREF} may change in this population. The constant T_{PREF} and T_{SET} range applied to analyses in the radio tagging study was collected over 11 days from August 28 - September 10, 2022: approximately 24% of the duration of the study period. As such, it was unlikely that the population-level T_{PREF} and T_{SET} range changed significantly over the study period. It is however interesting to note that during the 11 days that T_{PREF} was collected, the in-situ behavioural thermoregulation of Arctic grayling in the river was quite efficient. During this time, the T_{SET} range largely overlapped with available ambient river temperatures (hours 700-1000 on the inspection plots; Appendix 1) indicating that T_{SET} may have been impacted by the river temperature at the time of capture which dictated the starting temperature of the T_{PREF} experiments; Appendix 1). However, it is also not unreasonable to assume that the Arctic grayling allocate more effort to behavioural thermoregulation during these hot summer periods when temperatures in their foraging habitats exceed their preferred T_{SET} range.

Biologging with radio telemetry

Multiple factors came into play during the 2022 field season producing exceptionally noisy radio tag data which had to be cleaned before analysis. Industrial activity related to the Coastal Gaslink (CGL) pipeline, which had been ongoing in years prior, increased dramatically from past seasons in early August as operations in this region moved from pre-planning to pipe-laying. This upscaling in operations, which happened shortly after the initial definition and mapping of the study reaches, brought with it increased radio interference from industry activities and the accompanying near-constant radio chatter. These factors likely had a particular influence on radio tag signals in reach B, where the pipeline was being drilled underneath the Anzac River near the middle of the defined study reach and industry activity was the highest. Reach B, which was already prone to tag echo and collisions from the bedrock geomorphology, was also subject to more radio pings per second as a disproportionate number of tags were deployed in this reach (n = 41/50) as a function of the uneven distribution of Arctic grayling between the study reaches during the early season tagging window. Initial definition of reach B also included a 1-km section above the Anzac 'falls'. This chute obstruction, speculated for a time to be a barrier to Arctic grayling movements during low water years, occurs just upstream of some of the largest feeding congregations of Arctic grayling that we observed during this study and is a mere 300 meters below the site of the pipeline crossing. While it is now known that Arctic grayling do successfully travel up the chute in some years, initial snorkel surveys (conducted on August 2 and 4) didn't reveal any habitat use during the period we were defining study reaches in what appeared to be a potential low-water year. This, combined with unpredictable access to spur roads along CGL operational routes and the even one instance of being asked to leave the river ahead of blasting led us to the decision to truncate the upper bound reach B above the chute, but below the pipeline right-of-way. Further surveys indicated that large Arctic grayling were indeed occupying reaches above the right-of-way after August 16, but they were not included in this study. As a result of these cumulative factors, radio tag concentrations were particularly high in some of the noisiest parts of the study reaches.

The goal of this *in-situ* study was to capture a picture of an ecological system during a time when Arctic grayling behave territorially and as such are unlikely to leave the range of the receiver stations during the target data collection period. That 42 of 50 tags deployed produced useable data, a proportion that is relatively favorable by telemetry study standards, suggests that we achieved the goal of capturing this behavioral period. The fine-scale filter we used was inherently subjective, as tag signals must be interpreted as valid, erroneous, or from a tagged fish that has died, was depredated, or subject to early tag detachment. The most difficult cases of these to discern are detachments in which the tag falls off and begins transmitting environmental data instead of thermal habitat use data from the intended host. In this system where operational temperatures and environmental temperatures are often close together, a detached tag settling in an Arctic grayling-occupied habitat can be difficult to discern from a living fish using that same pool. For this reason, it is possible that the tags filtered out for detachment were underrepresented. We did, however, have repeat observations of tagged fish throughout the study and footage of a group of tagged fish together that provide evidence that the tags were staying on well, so we feel optimistic that these cases were rare if they happened (Figure 35).

Figure 35. Still picture from video footage showing three radio tagged Arctic grayling in reach B.

The vast majority of *VeDBA* detections were from small movements (95.5% of detections were between 0 - 0.2 on a scale to 1.5). This could be a result of Arctic grayling behavior as detected by the tri-axial accelerometer in the tag. During the snorkel study, Arctic grayling that were observed feeding would hold their position in the current and quickly dart up to forage before returning to their original position. These burst movements happened in a matter of seconds; events lasted a small proportion of the radio tag's 30-second averaging cycle for VeDBA and is smoothed by the remainder of the period's relatively small movements. It is likely that high activity bursts are underrepresented in the data. It is possible to interpret the *VeDBA* values recorded near zero as having some motion along the sway axis while very little activity would register along the surge or heave axes during

periods when Arctic grayling were holding their positions in the current (*sensu* Qasem et al. 2013). It would be possible to obtain higher-resolution *VeDBA* data if the tags were retrieved and manually downloaded, but over the course of this study we sampled over 70 Arctic grayling without a single recapture and the opportunity was not presented.

The calculated metric E_X showed that Arctic grayling exploited their preferred thermal habitats 81% of the time that it was available. This implies that over the study period, 19% of their time was spent operating outside of their T_{SET} range despite their preferred temperatures being available nearby. It is well understood in habitat ecology that an animal will exploit non-optimal habitats if the benefits of doing so outweigh the costs (Veech 2021). In this ecological snapshot, it is likely that feeding opportunities were drawing Arctic grayling away from their preferred thermal habitats during the day and/or that Arctic grayling were occupying warmer waters temporarily as a means to aid the efficiency of digestion (Armstrong et al. 2021).

Three major patterns in Arctic grayling thermoregulatory behaviors emerged in this study. For periods in which median ambient temperatures were fully within the T_{SET} range (e.g., study hours 0 - 250; Appendix 1), efficient thermoregulatory behavior was achieved frequently. This result is simple to interpret; when appropriate thermal habitats are abundant and are likely to overlap well with feeding habitats, they can be occupied at nearly all times. During a midseason warm spell when only nighttime temperatures were within T_{SET} (e.g., study hours 425 - 650; Appendix 1) thermoregulatory behavior was elevated during the day (with efficiency varying based on how far ambient temperatures deviated from T_{SET}), and Arctic grayling were less actively thermoregulating with respect to their thermal habitats at night when ambient temperatures were at or just above T_{SET} (a pattern visible, for example in tag 31, Appendix 1). This result would imply that during daytime feeding (the only time Arctic grayling feed as they are highly dependent on eyesight; Stamford et al. 2017), Arctic grayling sampled in this study were careful to spend adequate time in cooler temperatures to buffer the effects of warm ambient feeding temperatures. The opposite was true when only daytime temperatures were within T_{SET} during the cooler late season (e.g., after hour 850, ~September 4); Arctic grayling actively thermoregulated in warmer habitats at night and moved into unfavorably cool temperatures during the day to feed (visible well in tag 35, Appendix 1). These results also suggest that while Arctic grayling will avoid daytime temperature extremes during hot weather periods, they will not avoid unfavorably cool temperatures during the day as the season progresses. The observation that there is an uneven response to unfavourably cool temperatures and unfavourably warm temperatures can be considered in light of the variable effects of thermal stressors on fish. While the effects of cold temperature and shock in salmonids are important but understudied effects (Reid et al. 2021; Donaldson et al. 2008), the effects of high temperature extremes are well studied and can quickly become lethal (e.g. Jonsson 2023).

Further insights emerged in the GAMM analysis of how covariates additively influence thermoregulatory efficiency (Figure 32). The range of water temperatures associated with the strongest response in thermoregulatory efficiency, approximately 13-16 °C, is just

beyond the upper bound of the T_{SET} range of 13.1 °C. This indicates that Arctic grayling are most effective thermoregulators when their T_{SET} range is close to their thermal preference, and they can efficiently move between heterogeneous patches to thermoregulate while exploiting variable resource patches. The response in efficiency tails off as temperatures begin to exceed 16 °C, which indicates a decrease in how effectively Arctic grayling can thermoregulate as ambient temperatures move further away from the T_{SET} range and could also be interpreted as an indicator that diel feeding behaviors are altered during heat stress events.

The relationship between thermoregulatory efficiency and *VeDBA* is slightly less intuitive. The peak of the response curve between thermoregulatory efficiency and VeDBA (which serves as a proxy for energy expenditures in this study) occurs at VeDBA values close to 0.75; nearly six standard deviations above the mean recorded VeDBA across the population (0.12 ± 0.12). As VeDBA continued to increase, thermoregulatory efficiency decreased indicating a diminishing return on energy expenditure and efficiency. This suggests that effective thermoregulatory behavior is energetically costly to achieve for Arctic grayling during their summer rearing period, underscoring the importance of thermally heterogeneous rearing habitats. A small increase in thermoregulatory efficiency at very high values of VeDBA could possibly be attributed to more aggressive thermoregulation after large movements across warm riffle habitats connecting pools.

While the effects of habitat patchiness on thermoregulatory efficiency was weak, the top two AIC ranked index E models included habitat patchiness as a covariate. A possible explanation is that thermal habitat patchiness, a metric of aggregation of temperature patches, had an additive effect with temperature that together allowed for a model that better explained the variation in the data than temperature alone. Finally, the effects of fish body condition were uncertain as only the second model included it as a covariate while model AIC weights indicated it was of relative importance to explaining the variation in the data. While the effect size was small, there was a weakly positive relationship between thermoregulatory efficiency and body condition, indicating that fish with a healthier body condition were more efficient thermoregulators.

Challenges

Work with our collaborators in this study yielded some productive results. The collaboration with the John Hagen and Associates snorkel team allowed us to gather data on the availability of thermal habitats in the index reaches during their snorkel swims. The dates chosen for the riverscape drone survey were picked to coincide with these swims. These associations allowed us to create the riverscape-scale index of thermal habitat quality by pool. While we initially planned to analyze sediment as a limiting factor in collaboration with Alex Bevington and his team's sedimentation study in the Anzac River, the conditions of the river on our drone and snorkel dates were low and clear and the survey timing wasn't appropriate to detect any changes in Arctic grayling behavior based on sediment loading. As mentioned above, Arctic grayling are highly reliant on vision to feed (Stamford et al.

2017), and there were multiple events of sediment peaking which could have caused them to move to other locations, a known behavior we were hoping to capture. Indeed, after a rainfall event on August 28 our field notes read “river is mud!” and for the first time in the study we were unable to capture an Arctic grayling from reach B until conditions cleared (which they did, and successful angling resumed, though they cleared before the September 2 drone and snorkel surveys provided any opportunity to capture potential sediment-related behavioral changes). Considering the multiple stop-work orders issued to CGL over the summer of 2023 related to improper sediment control in the Anzac River (and others along its route; B.C. Environmental Assessment Office), this is a dimension of collaboration that would have yielded interesting results regarding limiting factors in this system.

In addition to the increased noise in the radio telemetry data, industry operations presented numerous logistical challenges. Both study reaches were accessible via spur roads off the Crocker FSR. Increased industry traffic on the Crocker dramatically slowed operations, with some days taking more than 3 hours to get one-way from our basecamp and field laboratory at Goose Lake to the study reaches. With some days demanding multiple trips between the field laboratory and the study sites (recall that all grayling used in this study were transported independently to the shuttlebox lab and released back into the Anzac River), there were at times very limited hours remaining for the crew of two to complete field objectives (e.g.(s): adding further sampling procedures to snorkel surveys to replicate the N-mixture methods in Hagen et al. 2021 (PEA-F23-F-3631); sampling an additional 10 Arctic grayling for establishing the T_{PREF} metric which was the most transport-involved objective; conducting night surveys to calibrate overnight thermal distributions; conducting further overland mapping surveys past Rkm 51 into the headwaters; more concerted radio tag tracking and recapture efforts).

In summary, this project set out to meet four primary objectives; to (1) identify critical Arctic grayling rearing habitats in the Anzac River through multiscale survey methods, (2) identify limiting factors that may impact Arctic grayling use of these habitats, (3) quantify the costs of behavioral thermoregulation in free-ranging Arctic grayling, and (4) forecast how further cumulative effects may alter the extents of these habitats. We found important relationships between Arctic grayling and pool habitats, in particular large pools with temperatures cooler than ambient river temperatures. We extended these findings to create an index highlighting areas of high importance related to these critical habitat metrics at the riverscape scale. We found that behavioral thermoregulation is energetically costly for the Anzac River Arctic grayling during their summer rearing period, and that these costs are associated with daily temperature variations which drive the diel distributions of their optimal thermal habitats. We found that Arctic grayling most carefully behaviorally thermoregulate when temperatures are near their T_{PREF} range and an analysis of median river temperature distributions against various cumulative warming scenarios found that habitats amenable to current thermal preference will decrease in extent to less than 1% of available habitats in the most extreme 1.5 °C scenario.

This research addressed monitoring needs outlined Action #9 in the Rivers Lakes, and Reservoirs Action Plan (*PEA.RLR.S03.Ri.09 Conduct research and monitoring on Arctic*

grayling) and provided a GIS indicator-based assessment of aquatic ecosystem health (priority gap 3 in Table 1 of Hagen & Stamford (2017)). The riverscape pool analysis and compilation of GIS layers that accompany this report provide a summary of critical Arctic grayling rearing habitats in the Anzac River at a scale sufficient for use by conservation managers seeking to affect positive change on this population (< 1 Rkm; Stamford et al. 2017). This together with insights derived from the reach-scale studies addressed aspects Steps 1-3 of the monitoring sequence in Hagen and Stamford (2017); acquired population data and indicators of aquatic ecosystem health for the purposes of delineating critical habitats and assessing conservation status, prioritized among candidate locations for conservation actions, and assessed potential future temperature-limiting factors operating within critical habitats in order design and initial conservation actions.

7. Recommendations

We base our recommendations to conservation planners on the pressures that the Anzac River Arctic grayling are likely to face over the coming years. As before, threats to this population can stem from overfishing, industry activity and habitat degradation, increased angling pressures along expanding road networks, and extreme temperature events (Stamford et al 2017; Lashmar and Ptolemy 2002). As currently managed since 1995, there is no harvest on this population, so the anticipated angling pressures this population will have to contend with are the well-documented physiological stressors associated with catch-and-release angling (Cooke et al. 2012). Along with stress responses to extreme heat events in freshwater fishes (Jonsson 2023) these physiological responses in fishes are mediated in both magnitude and duration by temperature. Access to suitable thermal habitats is essential for the long-term conservation of a population subjected to either of these pressures. As such, we recommend that, when possible, inseason management strategies should be used to close the recreational fishery during temperature extreme events within the latitude provided in the Provincial Fisheries Management Drought Response Plan (2019). To work with the nuances of resource management in a mixed-stock system, we also recommend educational signage be placed in high-traffic angling areas of the Anzac River detailing the effects of angling during heatwaves with readily accessible information akin to the messaging in the No-Fish-Dry-July campaign by the nonprofit organization Keep Fish Wet. We contend that signage educating about this populations of Arctic grayling, why there is no harvest, and discouraging angling during temperature extremes could have an effect among conservation-minded anglers in instances where management strategies are not tenable. As this watershed also supports blue-listed bull trout, this approach would extend benefits beyond just the focal species.

The use of long-term monitoring strategies are essential in stream ecosystems to allow researchers to monitor the progress of recovery efforts and assess the scale of impacts from disturbance events (Clements et al. 2021). Pools, river features which offer refuge from flow and temperature extremes - especially those downstream of features which produce high amounts of terrestrial drift - will always be of importance to the Anzac River Arctic

grayling. As a species, Arctic grayling have been suggested as an indicator species for shifting ecosystem health due to their sensitivity to disturbance and overfishing pressures (Cahill 2015). The encouraging report recently published by John Hagen and Associates finding that Arctic grayling populations have approximately doubled in the region over the past 25 years demonstrates the usefulness of long-term indices for conservation planning (FWCP Instagram post from August 2). As such, we recommend that a long-term index of thermal habitat quality by pool be developed for the Anzac River. While the full analysis undertaken in this report is not feasible to be replicated annually or semi-annually, the riverscape imaging process and pool distribution analysis can be conducted over a relatively short period of time (approximately three weeks or fewer for mapping, processing, and analysis depending on conditions). By pairing this index with the snorkel survey index, a paired, complementary dataset can be created that tracks Arctic grayling abundance against the availability of quality thermal habitats over time. Due to the shifting nature of the gravel-bed ecosystems in the Anzac River, we recommend this index be compiled between every five to ten years.

Finally, this study was proposed as a two-year study wherein these methods and analyses would be replicated in the Table River during year two. While it wasn't pursued in 2023 due to current logistical constraints and high industry activity in the area, it would be beneficial to pursue after the activity clears as the Table and Anzac Rivers together make up an important hub of Arctic grayling distributions in the region (Stamford et al. 2017). With the completion of the CGL pipeline and differences in river morphology, we would expect cleaner radio tag data to be produced from the Table River.

In summary, we recommend:

1. Where possible, explore management strategies to reduce angling pressures on Arctic grayling during thermal extremes,
2. Implement educational signage in the Anzac River discouraging anglers from stressing fish during thermal extremes, and provide pocket-thermometers at stations so anglers can make their own informed decisions,
3. Develop a long-term index of thermal habitat quality in the Anzac that can be efficiently and repeatedly conducted in this system over five to ten-year intervals, and
4. Extend these methods to examine the Table River to create a more complete picture of Arctic grayling habitat use and availability in this important region and replicate key metrics in the Table River alongside the Anzac River in future studies.

8. Acknowledgements

We gratefully acknowledge that this study took place on the overlapping traditional territories of Treaty 8 signatory Nations (Prophet River, Saulteau, and West Moberly First Nations) and on the traditional and unceded territory of the McLeod Lake Tse'Khene. We thank the FWCP for their generous financial support to complete this study. We thank Tom

Wilms for guidance on project workflows and a last-minute loan of a replacement drone while ours had to be sent back to the manufacturer for repairs. We thank Matt McLean, Meaghan Rupprecht, and Dr. Joseph Shea for vast amounts of advice, technical guidance, and assistance with drone image processing and GIS workflow development. We thank Dr. Nikolaus Ganter and the Omineca Fish Ambassadors Amber Pallister and Sydney Angielski for co-locating their field camp with ours and providing mutual logistical support and at times some light security to our field operations. We thank Liz Hirsch for help setting up and fine-tuning the shuttlebox field laboratory as well as sampling Arctic grayling. We thank Bryce O'Connor for technical planning help from his prior experience in the river (which saved us a lot of walking). We thank Chris Cena and Dr. Danie Erasmus for their guidance with the feasibility of integrating invertebrate density sampling into our sampling procedures. We thank Dr. Marc Pépino who shared his code with us to set up the initial heat transfer modeling framework. We thank Jesi Lauzon and Joel Khoo En for assistance with the field laboratory and initial processing of the reach-scale drone imagery. We thank Kari Van Ruskenveld for shuttling field technicians and volunteers between Prince George and the Anzac River valley and immense logistical aid. We thank OVERhang training for accommodating a special whitewater safety training session as well as a loaner drysuit while one of ours was being repaired for a broken zipper. We thank John Hagen and Associates for their mutual field support and wealth of knowledge and advice regarding this population and their mutual collaboration with us towards these goals. We thank Mike Stamford and Sue Pollard for helping us trace the history of the conservation status of this population. We thank the numerous people who helped us meet our tagging quotas by volunteering to come fishing with us; Matthew Blackburn, George Kenas, Kat Doucette, Meaghan Rupprecht, Brittney Reichert, Jesi Lauzon, and Liz Hirsch.

9. References

Abram, P. K., Boivin, G., Moiroux, J. & Brodeur. (2017). J. Behavioural effects of temperature on ectothermic animals: unifying thermal physiology and behavioural plasticity. Biol Rev 92, 1859–1876.

Armstrong, J. B., Fullerton, A. H., Jordan, C. E., Ebersole, J. L., Bellmore, J. R., Arismendi, I., Penaluna, B. E., & Reeves, G. H. (2021). The importance of warm habitat to the growth regime of cold-water fishes. Nature Climate Change, 11(4), 354–361. https://doi.org/10.1038/s41558-021-00994-y

B.C. Environmental Assessment Office (2023). Inspection record for Coastal GasLink Pipeline Project number 20230043_IR002.

Blouin-Demers, G., & Weatherhead, P. J. (2001). Thermal Ecology of Black Rat Snakes (elaphe Obsoleta) in a Thermally Challenging Environment. Ecology, 82(11), 3025–3043. https://doi.org/10.1890/0012-9658(2001)082[3025:TEOBRS]2.0.CO;2.

Cahill (2015). Alberta Environment and Parks and Alberta Conservation Association. 2015. Status of the Arctic Grayling (Thymallus arcticus) in Alberta: Update 2015. Alberta Environment and Parks. Alberta Wildlife Status Report No. 57 (Update 2015). Edmonton, AB. 96 pp.

Casas-Mulet, R., Pander, J., Ryu, D., Stewardson, M. J., & Geist, J. (2020). Unmanned aerial vehicle (Uav)-based thermal infra-red (Tir) and optical imagery reveals multi-spatial scale controls of cold-water areas over a groundwater-dominated riverscape. Frontiers in Environmental Science, 8, 64. https://doi.org/10.3389/fenvs.2020.00064

Chapman, B. B., Hulthén, K., Brodersen, J., Nilsson, P. A., Skov, C., Hansson, L.-A., & Brönmark, C. (2012). Partial migration in fishes: causes and consequences. Journal of Fish Biology, 81(2), 456–478. https://doi.org/10.1111/j.1095-8649.2012.03342.x

Cooke, S. J., Donaldson, M. R., O'connor, C. M., Raby, G. D., Arlinghaus, R., Danylchuk, A. J., Hanson, K. C., Hinch, S. G., Clark, T. D., Patterson, D. A., & Suski, C. D. (2013). The physiological consequences of catch-and-release angling: Perspectives on experimental design, interpretation, extrapolation and relevance to stakeholders. Fisheries Management and Ecology, 20(2–3), 268–287. https://doi.org/10.1111/j.1365-2400.2012.00867.x

Cooke, S. J., Martins, E. G., Struthers, D. P., Gutowsky, L. F. G., Power, M., Doka, S. E., Dettmers, J. M., Crook, D. A., Lucas, M. C., Holbrook, C. M., & Krueger, C. C. (2016). A moving target—incorporating knowledge of the spatial ecology of fish into the assessment and management of freshwater fish populations. Environmental Monitoring and Assessment, 188(4), 239. https://doi.org/10.1007/s10661-016-5228-0

Christensen, E. A. F., Andersen, L. E. J., Bergsson, H., Steffensen, J. F., & Killen, S. S. (2021). Shuttle-box systems for studying preferred environmental ranges by aquatic animals. Conservation Physiology, 9(1), coab028. https://doi.org/10.1093/conphys/coab028

Christian, K. A., & Weavers, B. W. (1996). Thermoregulation of monitor lizards in australia: An evaluation of methods in thermal biology. Ecological Monographs, 66(2), 139–157. https://doi.org/10.2307/2963472

Clements, W. H., Herbst, D. B., Hornberger, M. I., Mebane, C. A., & Short, T. M. (2021). Long-term monitoring reveals convergent patterns of recovery from mining contamination across 4 western US watersheds. Freshwater Science, 40(2), 407–426. https://doi.org/10.1086/714575

Crook, D. A. (2004). A method for externally attaching radio transmitters to minimize dermal irritation. Journal of Fish Biology, 64(1), 258–261. https://doi.org/10.1111/j.1095-8649.2004.00282.x

Dugdale, S. J., Kelleher, C. A., Malcolm, I. A., Caldwell, S., & Hannah, D. M. (2019). Assessing the potential of drone-based thermal infrared imagery for quantifying river temperature heterogeneity. Hydrological Processes, 33(7), 1152–1163. https://doi.org/10.1002/hyp.13395

Dzara, J. R., Neilson, B. T., & Null, S. E. (2019). Quantifying thermal refugia connectivity by combining temperature modeling, distributed temperature sensing, and thermal infrared imaging. Hydrology and Earth System Sciences, 23(7), 2965–2982. https://doi.org/10.5194/hess-23-2965-2019

Elsner, R. A., & Shrimpton, J. M. (2019). Behavioural changes during the parr–smolt transformation in coho salmon Oncorhynchus kisutch : is it better to be cool? Journal of Fish Biology, jfb.14069. https://doi.org/10.1111/jfb.14069

Farrell, A. P. *et al*. Pacific Salmon in Hot Water: Applying Aerobic Scope Models and Biotelemetry to Predict the Success of Spawning Migrations. Physiol Biochem Zool 81, 697–709 (2008).

Fausch, K. D., Torgersen, C. E., Baxter, C. V., & Li, H. W. (2002). Landscapes to Riverscapes: Bridging the Gap between Research and Conservation of Stream Fishes. BioScience, 52(6), 483. https://doi.org/10.1641/0006-3568(2002)052[0483:LTRBTG]2.0.CO;2

Fieberg, J., Signer, J., Smith, B., & Avgar, T. (2021). A 'How to' guide for interpreting parameters in habitat-selection analyses. Journal of Animal Ecology, 90(5), 1027–1043. https://doi.org/10.1111/1365-2656.13441

FWCP. (2020). Peace Region Rivers, Lakes, & Reservoirs Action Plan.

Hagen, J., and M. Stamford. 2023. Parsnip Arctic Grayling Critical Habitats and Abundance: 2018-2022 Final Report. Report prepared for the Fish and Wildlife Compensation Program – Peace Region, Prince George, BC. FWCP Project No. PEA-F23-F-3631.

Hagen, J., and Stamford, M. (2017). FWCP Arctic grayling monitoring framework for the Williston Reservoir Watershed. Report prepared for the Fish and Wildlife Compensation Program – Peace Region

Hagen, J. & Gantner, N. (2019) Abundance and trend of Arctic grayling (Thymallus arcticus) in index sites of the Parsnip River watershed, 1995-2019. FWCP Report. Project No. PEA-F20-2959

Hauer, F. R., Locke, H., Dreitz, V. J., Hebblewhite, M., Lowe, W. H., Muhlfeld, C. C., Nelson, C. R., Proctor, M. F., & Rood, S. B. (2016). Gravel-bed river floodplains are the ecological nexus of glaciated mountain landscapes. Science Advances, 2(6), e1600026. https://doi.org/10.1126/sciadv.1600026

Hawkshaw, S.C.F. and J.M. Shrimpton. 2014. Temperature preference and distribution of juvenile Arctic grayling (Thymallus arcticus) in the Williston Watershed, British Columbia, Canada. Fish and Wildlife Compensation Program – Peace Region Report No. 366. 40 pp plus appendices

Hesselbarth, M.H.K., Sciaini, M., With, K.A., Wiegand, K., Nowosad, J. 2019. landscapemetrics: an open-source R tool to calculate landscape metrics. - Ecography 42:1648-1657 (v0.0).

Hijmans R (2023). _terra: Spatial Data Analysis_. R package version 1.7-3, <https://CRAN.R-project.org/package=terra>.

Hughes, N. F. (1992a). Ranking of Feeding Positions by Drift-Feeding Arctic Grayling (Thymallus arcticus) in Dominance Hierarchies. Canadian Journal of Fisheries and Aquatic Sciences, 49(10), 1994–1998. https://doi.org/10.1139/f92-222

Hughes, N. F. (1992b). Selection of Positions by Drift-Feeding Salmonids in Dominance Hierarchies: Model and Test for Arctic Grayling (Thymallus arcticus) in Subarctic Mountain Streams, Interior Alaska. Canadian Journal of Fisheries and Aquatic Sciences, 49(10), 1999–2008. https://doi.org/10.1139/f92-223

Hughes, N. F. (1998). A Model of Habitat Selection by Drift-Feeding Stream Salmonids at Different Scales. Ecology, 79(1), 281–294. https://doi.org/10.1890/0012-9658(1998)079[0281:AMOHSB]2.0.CO;2

Hughes, N. F. (1999). Population processes responsible for larger-fish-upstream distribution patterns of Arctic grayling (Thymallus arcticus) in interior Alaskan runoff rivers. Canadian Journal of Fisheries and Aquatic Sciences, 56(12), 2292–2299. https://doi.org/10.1139/f99-157

Johnson, C. J., Nielsen, S. E., Merrill, E. H., McDonald, T. L., & Boyce, M. S. (2006). Resource selection functions based on use-availability data: Theoretical motivation and evaluation methods. The Journal of Wildlife Management, 70(2), 347–357. https://www.jstor.org/stable/3803680

Jonsson, B. (2023). Thermal effects on ecological traits of salmonids. Fishes, 8(7), 337. https://doi.org/10.3390/fishes8070337

Lele SR, Keim JL, Solymos P (2019). _ResourceSelection: Resource Selection (Probability) Functions for Use-Availability Data_. R package version 0.3-5, <https://CRAN.R-project.org/package=ResourceSelection>.

Lele, S. R. & Keim, J. L. (2006) Weighted distributions and estimation of resource selection probability functions. Ecology 87, 3021–3028.

Martins, E. G., Hinch, S. G., Patterson, D. A., Hague, M. J., Cooke, S. J., Miller, K. M., Lapointe, M. F., English, K. K., & Farrell, A. P. (2011). Effects of river temperature and climate warming on stock-specific survival of adult migrating Fraser River sockeye salmon (Oncorhynchus nerka). Global Change Biology, 17(1), 99–114. https://doi.org/10.1111/j.1365-2486.2010.02241.x

McPhail, J.D. 2007. The freshwater fishes of British Columbia. The University of Alberta Press, Edmonton, Alberta.

Morash, A. J., Speers-Roesch, B., Andrew, S., & Currie, S. (2021). The physiological ups and downs of thermal variability in temperate freshwater ecosystems. Journal of Fish Biology, 98(6), 1524–1535. https://doi.org/10.1111/jfb.14655

Nakano, S., Kitano, S., Nakai, K., & Fausch, K. D. (1998). Competitive interactions for foraging microhabitat among introduced brook charr, Salvelinus fontinalis, and native bull charr, S. confluentus, and westslope cutthroat trout, Oncorhynchus clarki lewisi, in a Montana stream. Environmental Biology of Fishes, 52(1–3), 345–355. https://doi.org/10.1023/A:1007359826470

Pebesma, E., 2018. Simple Features for R: Standardized Support for Spatial Vector Data. The R Journal 10 (1), 439-446, https://doi.org/10.32614/RJ-2018-009

Pebesma, E., & Bivand, R. (2023). Spatial Data Science: With Applications in R (1st ed.). Chapman and Hall/CRC. https://doi.org/10.1201/9780429459016

Qasem, L., Cardew, A., Wilson, A., Griffiths, I., Halsey, L. G., Shepard, E. L. C., Gleiss, A. C., & Wilson, R. (2012). Tri-axial dynamic acceleration as a proxy for animal energy expenditure; should we be summing values or calculating the vector? PLoS ONE, 7(2), e31187. https://doi.org/10.1371/journal.pone.0031187

Reid, C. H., Patrick, P. H., Rytwinski, T., Taylor, J. J., Willmore, W. G., Reesor, B., & Cooke, S. J. (2022). An updated review of cold shock and cold stress in fish. Journal of Fish Biology, 100(5), 1102–1137. https://doi.org/10.1111/jfb.15037

Rezende, E. L., Castañeda, L. E., & Santos, M. (2014). Tolerance landscapes in thermal ecology. Functional Ecology, 28(4), 799–809. https://doi.org/10.1111/1365-2435.12268

Sears, M. W., Riddell, E. A., Rusch, T. W., & Angilletta, M. J. (2019). The World Still Is Not Flat: Lessons Learned from Organismal Interactions with Environmental Heterogeneity in Terrestrial Environments. Integrative and Comparative Biology, 59(4), 1049–1058. https://doi.org/10.1093/icb/icz130

Stanford, J. A., Lorang, M. S., & Hauer, F. R. (2005). The shifting habitat mosaic of river ecosystems. SIL Proceedings, 1922-2010, 29(1), 123–136. https://doi.org/10.1080/03680770.2005.11901979

Stamford and Pollard (2022). Personal communications. A series of emails explaining the history of Parsnip watershed Arctic grayling conservation status with relation to the use of Conservation Units in B.C.

Stamford, M., J. Hagen, and S. Williamson. 2017. Limiting Factors, Enhancement Potential, Conservation Status, and Critical Habitats for Arctic Grayling in the Williston Reservoir Watershed, and Information Gaps Limiting Potential Conservation and Enhancement

Actions. Report prepared for the Fish and Wildlife Compensation Program – Peace Region, Fort St. John, BC.

Stamford, M, and Taylor, E.B. 2004. Phylogeographical lineages of Arctic grayling (Thymallus arcticus) in North America: divergence, origins, and affinities with Eurasian Thymallus. Molecular Ecology.

Torgersen, C. E., Le Pichon, C., Fullerton, A. H., Dugdale, S. J., Duda, J. J., Giovannini, F., Tales, É., Belliard, J., Branco, P., Bergeron, N. E., Roy, M. L., Tonolla, D., Lamouroux, N., Capra, H., & Baxter, C. V. (2022). Riverscape approaches in practice: Perspectives and applications. Biological Reviews, 97(2), 481–504. https://doi.org/10.1111/brv.12810

Troia, M. J., Kaz, A. L., Niemeyer, J. C., & Giam, X. (2019). Species traits and reduced habitat suitability limit efficacy of climate change refugia in streams. Nature Ecology & Evolution, 3(9), 1321–1330. https://doi.org/10.1038/s41559-019-0970-7

Vannote, R. L., Minshall, G. W., Cummins, K. W., Sedell, J. R., & Cushing, C. E. (1980). The river continuum concept. Canadian Journal of Fisheries and Aquatic Sciences, 37(1), 130–137. https://doi.org/10.1139/f80-017

Vatland, S. J., Gresswell, R. E., & Poole, G. C. (2015). Quantifying stream thermal regimes at multiple scales: Combining thermal infrared imagery and stationary stream temperature data in a novel modeling framework. Water Resources Research, 51(1), 31–46. https://doi.org/10.1002/2014WR015588

Wich, S. A., & Koh, L. P. (2018). Conservation drones (Vol. 1). Oxford University Press. https://doi.org/10.1093/oso/9780198787617.001.0001

Wilms, T., & Whitworth, G. (2016). Mapping of critical summer thermal refuge habitats for chinook salmon, coho salmon, steelhead and bull trout in the Nicola River Watershed – 2016 (Habitat Stewardship Program for Species at Risk project reference number: 2016HSP7592).

Wilms, T. (2022). Personal communications. A series of phone calls giving advice about drone workflows and methodologies.

Wolkovich, E. M., Cook, B. I., McLauchlan, K. K., & Davies, T. J. (2014). Temporal ecology in the Anthropocene. Ecology Letters, 17(11), 1365–1379. https://doi.org/10.1111/ele.12353

Xie, Y. (2013). animation: An R Package for Creating Animations and Demonstrating Statistical Methods. Journal of Statistical Software, 53(1), 1-27. https://doi.org/10.18637/jss.v053.i01